JOURNAL OF Materials CHEMISTRY
Feature Article

Heterogenous events in the crystallization of zeolites

David P. Serrano and Rafael van Grieken

School of Experimental Sciences and Technology, Rey Juan Carlos University, 28933 Móstoles, Madrid, Spain. E-mail: dserrano@escet.urjc.es; rvangrieken@escet.urjc.es

Received 23rd January 2001, Accepted 16th July 2001
First published as an Advance Article on the web 7th September 2001

While for many years zeolite crystallization has been assumed to proceed mainly through solution-mediated transformations, recent works point towards the presence of heterogeneous events in both nucleation and crystal growth steps. When the zeolite synthesis starts from a solid-containing gel, the participation of the amorphous raw phase in the formation of the zeolite nuclei has been clearly established. Moreover, in some cases the zeolite crystals grow by reorganization of the hydrogel through solid–solid transformations. In zeolite synthesis starting from clear solutions, the crystallization mechanism has been recently studied by *in situ* light scattering techniques, showing the formation in the first stages of an X-ray amorphous gelatinous phase, consisting of particles with sizes below 10 nm. These nanoparticles seem to be involved directly in the crystallization, as their aggregation and subsequent densification have been proposed to lead to the formation of the zeolite crystals. The crystallization of zeolites through heterogeneous *versus* homogeneous pathways is favoured at high solid concentrations or when the solubility of the silicate species is low, as occurs during zeolite synthesis through the fluoride route.

1. Introduction

According to the classical definition, zeolites are microporous crystalline aluminosilicates. The term zeolite was coined by a Swedish mineralogist, A. Cronstadt, in 1756 applied to the mineral stilbite, with the meaning of boiling stone, as this material seemed to boil when heated due to its high water content.[1] Thereafter, a large variety of naturally occurring zeolites were identified and characterized. Many of these natural zeolites were further synthesized in the laboratory, whereas new structures and compositions were discovered that did not have counterparts in nature. In the last 50 years, a number of zeolites (X, Y, A, ZSM-5, *etc.*) have found commercial applications.[2]

The presence of strong acid sites, associated with the Al atoms, and the uniformity of pore sizes in zeolites provide these materials with unique properties (high activity and shape selectivity) for their use in heterogeneous catalysis, adsorption and ion exchange operations. Zeolites are usually referred to as molecular sieves, since they may discriminate among different molecules having slight variations in molecular size. The progress in zeolite synthesis has led to the preparation of new structures, often with increased pore diameters in order to enlarge the size of the molecules that are able to enter and diffuse through the zeolite channels and cavities. At present, the number of zeolite structures approved by the International Zeolite Association (IZA) is over 130. Moreover, the properties of "zeolitic materials" have been widened by the discovery in 1992 of the MCM-41 family of zeolite-like amorphous solids, characterized by having uniform and ordered pore systems within the mesopore range.[3]

Huge advances have been also achieved regarding the chemical composition of zeolites. Currently, many structures can be prepared as silicalites having no aluminium, which turns them into hydrophobic materials. Moreover, a variety of metals have been successfully incorporated into zeolite frameworks, usually replacing the aluminium atoms, such as Ti, B, Ga, Fe, Cr, V, Mn, Zr, Zn, *etc.* On the other hand, other families of microporous materials, such as aluminophosphates and metalloaluminophosphates have been synthesized exhibiting properties and structures closely related to those of zeolites. As a consequence of these achievements, the above quoted classical definition of zeolites is no longer applied. Instead, the term zeolitic materials is now commonly used to cover both conventional and new structures and compositions.

Zeolites are usually crystallized under hydrothermal conditions, at basic pH and at temperatures in the range 60–200 °C, from gels containing the silica and alumina sources, basic agents and alkali metal cations. In many cases, the zeolite synthesis requires also the presence of organic compounds (quaternary ammonium salts, amines, alcohols, *etc.*), that may play the role of pore filling agents or may act as templates that direct the crystallization towards the formation of a specific structure. Recent progress in zeolite synthesis includes the use of solvents different from water, heating by microwave radiation, preparation of zeolite films and membranes on different supports, *etc.*

In spite of the advances in the synthesis and applications of zeolites, their mechanism of crystallization is still not well understood. In fact, it has been a matter of controversy during the last 20 years. Two extreme alternatives have been considered in the past to explain the nucleation and growth of zeolite crystals.[4] In the first approach (homogeneous mechanism), the nucleation is supposed to occur directly from the liquid phase and, once the nuclei reach a critical size becoming successful nuclei, they grow into crystals by the progressive incorporation of soluble species. According to this mechanism, the role of amorphous solid phases, if present, is simply as a reservoir of nutrients, being removed as the growth of the crystals from the solution progresses. In the second alternative (heterogeneous mechanism), it is assumed that the zeolite crystallization proceeds by the reorganization of an amorphous solid phase, usually referred to as the hydrogel, that it is present at the beginning of the synthesis. Therefore, in this approach, nucleation takes place within the hydrogel and the crystals are formed by solid–solid transformations.

Different alternatives have been postulated attempting to conciliate these two 'extreme' mechanisms. One of the most widely accepted ideas assumes that nucleation is closely related to the hydrogel, occurring at the surface or within the amorphous particles, whereas the crystal growth step is considered to be a solution mediated process, taking place by the incorporation of soluble species around the nuclei.[5] However, recent studies carried out with both *ex situ* and *in situ* techniques suggest that zeolite crystallization proceeds in many cases through heterogeneous phenomena in both nucleation and crystal growth steps. It seems clear that there is not a general mechanism which can explain all zeolite crystallizations, as a consequence of the high variety of structures, compositions and synthesis conditions that may occur.

However, from the most recent literature results it arises that, in many zeolite syntheses, nucleation and crystal growth proceed through heterogeneous transformations involving amorphous and/or pseudocrystalline particles.

The present review covers mainly work appearing in recent years pointing out the possible presence of heterogeneous events during zeolite synthesis. These works have been classified according to the features of the raw gel, as this may strongly determine the type of crystallization mechanism. The first section deals with those systems having an amorphous solid phase in the raw synthesis mixture, which may favour the development of heterogeneous transformations. The second part of this review is devoted to those zeolite crystallizations starting from clear solutions, without any macroscopic evidence of the presence of solid phases.

2. Zeolite crystallization from solid-containing gels

Most conventional zeolite syntheses of commercial value use as starting materials amorphous gel phases with a high solid content, which leads to high product yields. Generally, these gels are formed by the mixing at basic pH of silicate and aluminate solutions in which the source of the silicon and aluminium atoms may be polymeric or monomeric. As the synthesis proceeds at temperatures in the range 60–200 °C, some gel dissolution occurs depending on the operation conditions, whereas a crystalline phase starts building up after an induction period. The presence of a high number of different oligomeric aluminosilicate species participating in the formation of the crystalline phase leads to a very complex system, which is difficult to describe simply by only one mechanism of crystallization. Nevertheless, in the synthesis starting from a solid-like gel precursor, the contribution of heterogeneous events has been clearly shown through different experimental evidences that are described and discussed below.

Jacobs, Derouane and Weitkamp[6] in 1981 reported the synthesis of X-ray amorphous (XRA) "zeolites" which exhibited catalytic properties typical for ZSM-5 materials. The crystallization, studied between 6 hours and 10 days, was carried out in the presence of tetrapropylammonium (TPA) ion as template. The crystallinity measured by IR spectroscopy (skeletal vibration at 550 cm^{-1}) showed a totally different behaviour than the sigmoidal plot obtained for the changes in the X-ray diffraction (XRD) crystallinity. IR spectroscopy was able to identify crystalline order for crystals with less than 4 unit cells. The X-ray crystallinity indicated an induction–nucleation period followed by a growth period typical of a conventional crystallization mechanism, a behavior completely different from that shown by IR spectroscopy. These XRA samples were loaded with Pt and tested in the hydroconversion of *n*-decane and compared with highly crystalline samples of zeolites ZSM-5 and Y, exhibiting catalytic activity very similar to that of crystalline ZSM-5. The authors suggested the presence of very small crystals (<8 nm) imbedded in an amorphous silica–alumina matrix to explain the catalytic results. Interestingly, the first sample (crystallization kinetics obtained after 6 hours, X-ray amorphous), showed an IR crystallinity of $>60\%$ with catalytic properties clearly higher than those exhibited by an amorphous silica–alumina catalyst prepared as a reference sample.

Perhaps one of the main contributions to clarify the role of the different variables involved in the synthesis of pentasil zeolites was made by Derouane, Gabelica and coworkers[7,8] during the 1980s. They postulated two extreme synthesis mechanisms governing the formation and growth of ZSM-5 crystallites in the presence of TPA as structure-directing agent, depending on the source of silica and the relative concentration of the reactants. Syntheses starting from silica solutions (type A) with low Si/Al and Na^+/SiO_2 ratios were found to take place by liquid phase ion transportation, whereas syntheses starting from aqueous silicate solutions (type B), with higher Si/Al and Na^+/SiO_2 ratios, appeared to be governed by a solid hydrogel reconstruction.

Fig. 1 shows a schematic representation of both types of mechanisms. Mechanism A essentially occurs in highly alkaline medium, where the solubility of polymeric silicate ions is increased. In this case, depolymerization of the silica source to yield the appropriate building blocks, is the rate-limiting step. The resulting monomeric or oligomeric silicate anions can either condense with aluminate species to form aluminosilicate complexes or interact directly with TPA^+ ions, the latter being capable of ordering around them (preferably Si-richer silicate units) to form stable nuclei. The preference to accommodate silica instead of alumina by the ZSM-5 nuclei leads to an increase in the crystal growth rate at the expense of the nucleation rate from dissolved silicate species in solution. The gel dissolution supplies the reactants for the process, balancing the thermodynamic equilibrium of the complex system. As the silicate species available in solution are exhausted, the gel continues to dissolve and bring progressively Al-rich soluble species to the outer layer of the growing particles. This mechanism yields large crystals with an inhomogeneous Al distribution.

According to mechanism B, starting from an aqueous sodium silicate solution, the ingredients are mixed at acidic pH whereas the hydrogel formation at pH = 11 takes place through NaOH addition. In this case, the starting solution contains monomeric or low oligomeric silica species since the presence of silicate ions is not limited by any depolymerization process, the solution composition being very similar to the reagent ratio. The high Si/Al and Na^+/SiO_2 molar ratios favor a rapid nucleation through the interaction of the structure directing TPA^+ cations, present throughout the gel, with the reactive aluminosilicate anions. Under these conditions, a direct recrystallization process is postulated involving mainly a solid hydrogel transformation, as suggested by the absence of low molecular weight species in the analysis of the solution by liquid ^{29}Si NMR. Studies of the syntheses of zeolites Y and mordenite[9] further confirmed such a mechanism. Indeed, a rapid crystal growth yields a large number of small crystallites with a homogeneous Al radial distribution. The analysis of the Si/Al molar ratios during the whole crystallization process shows a remarkably constant value indicating that both the growing crystallites and their gel precursor must continuously keep the same composition, supporting the direct hydrogel transformation mechanism through internal rearrangements.

The above quoted reports can be considered as the starting point of a scientific debate concerning the existence of heterogeneous transformations during zeolite crystallizations that has been enriched in recent years by outstanding contributions.

2.1. Crystallization of aluminium-containing zeolites

Among the different factors affecting zeolite formation, it is widely accepted that the composition and structure of the starting aluminosilicate gels influence their hydrothermal treatment and, therefore, the properties of the zeolite formed. Thus, one of the main topics in the study of the mechanism governing zeolite formation has been the characterization of the aluminosilicate gel prior to hydrothermal treatment and the relationship between its properties and the crystallization process.

The role of alkali metal cations in the properties of the aluminosilicate gels used as starting materials in the synthesis of zeolites has been investigated through different spectroscopic techniques. Ivanova *et al.*[10] studied by multinuclear NMR the aluminosilicate phase obtained upon mixing clear alkali-silicate and aluminate solutions, and found that tetrahedrally coordinated Al was homogeneously dispersed in the gel, irrespective of the nature of the alkali metal cation. Nevertheless, the textural properties of the gels estimated by ^{129}Xe NMR spectroscopy, showed a clear dependence on the

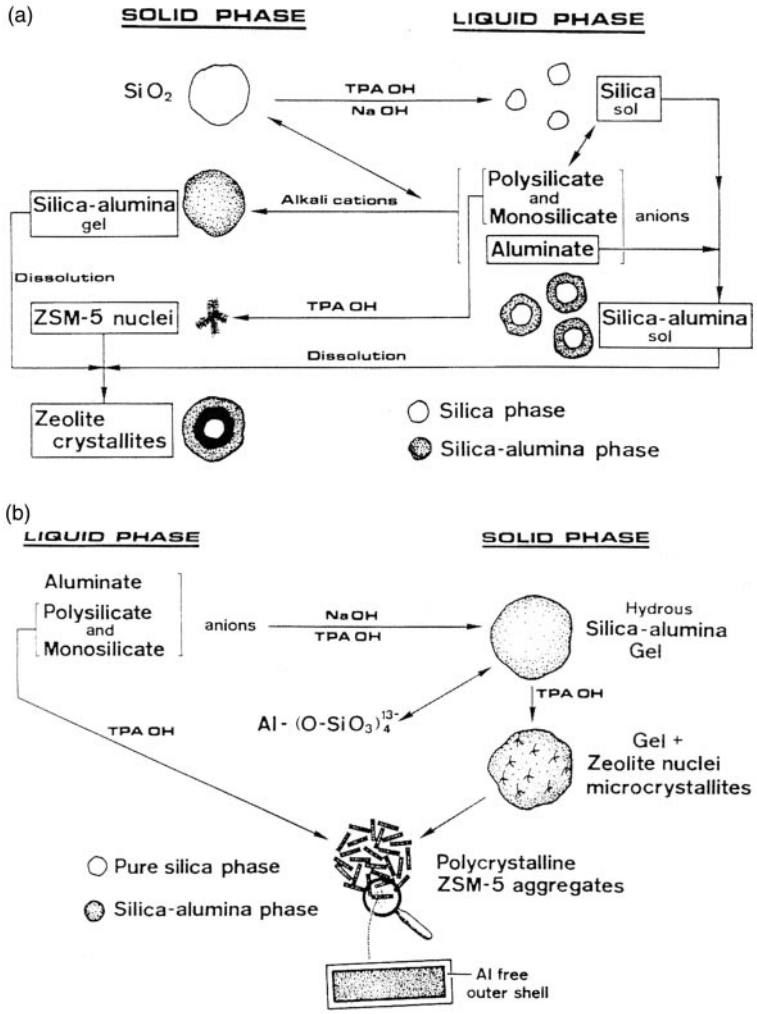

Fig. 1 Zeolite crystallization mechanisms: (a) solution mediated process (type A); (b) hydrogel reconstruction (type B). Reprinted with permission from reference 7.

type of alkali metal cation present in the materials. Similarly, Subotic *et al.*[11] postulated the existence of structural subunits inside the X-ray amorphous matrix with sizes in the range 5–20 nm, which resemble those shown by the crystalline products when "structure-forming" Na^+ ions are present in the synthesis mixture. When K^+ is used, or the Na^+ gel is heated at 500 °C, the number of structural subunits is considerably lower, as estimated by the electron diffraction patterns of the solids, which clearly affects the rate of hydrothermal transformation of the X-ray amorphous solids into crystalline product.

Nagy *et al.*[12] studied the physicochemical and structural properties of aluminosilicate gels obtained by mixing an $Al(OH)_3$ solution with fumed silica, typically used in zeolite syntheses as starting materials. The gel composition was varied to determine the role of the structure-directing agents (tetraalkylammonium ions, TAA^+) in the preparation of the aluminosilicate gels under different synthesis conditions. When TAAOH is used in the absence of Na^+ cations (gel II), tetrahedral Al atoms are well dispersed within the gel structure and the well-hydrated TAA^+ cations act as counter cations of the negatively charged gel. When the tetralkylammonium cation is added as its bromide salt at neutral pH (gel I), the Al atoms are not very well dispersed throughout the gel, and medium (21 Å) and large (40–60 Å) cavities are detected, probably related to TAABr crystallites. In the presence of TAABr and NaOH (gel IV), the Al is better dispersed but the counter cations are essentially sodium ions, leading to less dispersion of the TAA^+ cations within the gel. The characterization of the textural properties of such gels by means of ^{129}Xe NMR indicates the high dispersion of the structure-directing agent when TAAOH is used during the gel formation, suggesting a direct role of the monomerically dispersed TAA species in the zeolite synthesis.

Aging of the starting gel is another feature closely related to the nucleation step in the synthesis of zeolites. Bell and coworkers[13] studied the effect of aging on the synthesis of NaY zeolite using colloidal silica and sodium aluminate solutions as starting materials. As illustrated in Fig. 2, they found an acceleration of the crystallization kinetics and a decrease in the crystal size with aging, especially for aging times up to 12 h, consistent with the generally accepted hypothesis that aging enables the formation of nuclei from which crystals subsequently grow. The high pH and high Al content of the solution during the first 12 h of aging lead to the formation of an amorphous aluminosilicate with Si/Al = 1 and Na/Al = 2. It is proposed that this solid phase coexists with silica until the mixture is heated and the silicate anions released in the solution react with a portion of the solid aluminosilicate to produce NaY nuclei. The high concentration of hydrated Na^+ cations in the amorphous aluminosilicate seems to stabilize the faujasite structure. The portion of the aluminosilicate not involved in the formation of NaY nuclei reacts with the Si-rich solution to form a different aluminosilicate with higher Si/Al ratio used in the synthesis as a feedstock for crystal growth.

After gel formation and aging, nucleation is the subsequent stage in a conventional crystallization process before crystal growth. Among the different theories on the origin of the zeolite nuclei, a relevant contribution to support the existence

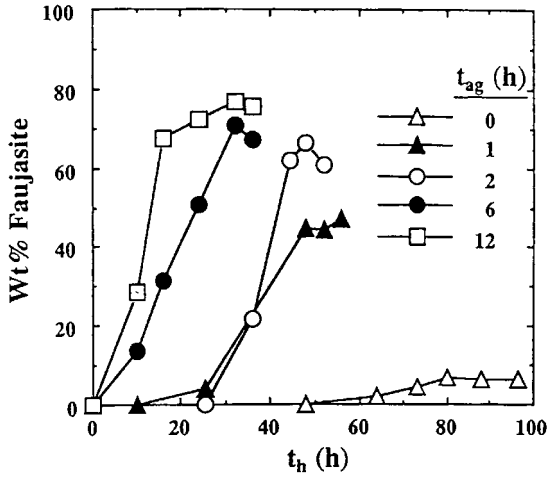

Fig. 2 Effect of aging on the synthesis of zeolite NaY: wt% of zeolite in the solid phase as a function of the heating time (t_h) for different aging times (t_{ag}). Reprinted with permission from reference 13.

of non-mediated solution nucleation processes was developed by Subotic *et al.*,[14,15] based on a previous work by Zhdanov.[16] The first part of the gel–crystal transformation followed an exponential dependence with the synthesis time in which the nucleation rate was increased during the crystallization process. It was postulated that the crystallization nuclei were not only those aluminosilicate polymers formed in the liquid phase, but also similar entities having ordered structure (quasi-crystalline zeolite) surrounded by amorphous polymer in the gel. According to these authors, their growth is not possible inside the gel phase but may take place when the gel dissolves during the progress of the crystallization. They concluded that the crystallization of ZSM-5 could be adequately explained following a model where the nucleation takes place either at the external surface of the gel (classical heterogeneous nucleation) or in inner pockets of the gel (autocatalytic nucleation). What was clearly excluded was the contribution of homogeneous nucleation under the usual synthesis conditions since the supersaturation present in most of zeolite syntheses would lead to much longer times for the appearance of the first crystalline nuclei.[17] Certain experimental evidence, such as the increasing rate of nuclei formation, the large portion of fine particles detected in the crystalline end-product or the influence of gel aging on the crystallization process, cannot be easily explained by a surface heterogeneous nucleation, suggesting that a contribution from autocatalytic nucleation exists during zeolite crystallization from gels.

Thompson *et al.*[18,19] modified the conclusions obtained in the previous works[14,15] since they noted that nucleation begins very early in the synthesis process in spite of the low fraction of crystals formed by the heterogeneous nucleation mechanism. Moreover, the nucleation of all crystals was essentially complete before the ZSM-5 crystallinity had reached 10%. This result was not expected as more than 95% of the nuclei were still contained in the amorphous gel and were not released until the remaining 90% of the amorphous gel was dissolved. To better predict earlier nucleation rates, an empirical modification of the original autocatalytic nucleation hypothesis was made, assuming that the nuclei were located preferentially near the outer surface of the amorphous gel particles. The results from this model were consistent with several experimental data and, although the good fitting did not prove unequivocally the conceptual validity of the model, at least it allows the existence of nuclei sources different from the solution (homogeneous nucleation) or solid surface (classical heterogeneous nucleation) to be postulated.

A noteworthy feature related to the existence of a solid–solid transformation is the non-aqueous synthesis of molecular sieves. Wenyang *et al.*[20] have studied the preparation of zeolites ZSM-35 and ZSM-5 by mixing an appropriate amount of an anhydrous gel (calcined at 823 K), obtained from mixing an acidic sodium silicate solution and a basic aluminium sulfate solution, and a mixture of ethylenediamine and triethylamine. The ratio of the different species in the synthesis mixture determines not only the possibility of obtaining crystalline products but also the different crystalline phases being formed. Thus, controlling the mol% of triethylamine and SiO_2 is a key factor to select ZSM-35 or ZSM-5 as product. Throughout the crystallization, neither SiO_2 and Al_2O_3 dissolved in the amine mixture and the SiO_2/Al_2O_3 molar ratio was constant in the solid, thus supporting a solid phase transformation. Other zeolite structures, such as ZSM-48, have been also obtained through the solid–solid transformation mechanism in the absence of water, where the type of alkali metal chloride plays a crucial role in the synthesis.[21] The introduction of alkali metal chlorides different from NaCl greatly slows down the crystallization rates showing its role as structure-directing agent, shortening the induction period and increasing the crystallization rate. The use of different alkali metal chlorides also influences the morphology and the particle size of the ZSM-48 zeolite but not the bulk SiO_2/Al_2O_3 ratio of the crystalline product, in accord with the heterogeneous crystallization mechanism governing the process.

Another piece of work relevant for supporting the existence of solid–solid transformation in zeolite synthesis has been carried out by the use of the vapor-phase transport (VPT) method. Xu *et al.*[22] first reported that an aluminosilicate dry gel was transformed into a zeolite with MFI topology by contact with water and amine vapors. The amorphous gel obtained by mixing aluminium sulfate, sodium silicate and sodium hydroxide was placed in a sieve-bottomed container, placed on top of a supporting device inside an autoclave, as shown in Fig. 3. An ethylenediamine–triethylamine aqueous solution was placed in the bottom of the autoclave, avoiding any direct contact between the gel and the solution. The powder diffraction patterns of the resulting samples showed the MFI topology, even for a completely dried gel. The composition of the ZSM-5 samples was analogous to the gel composition, suggesting a solid-phase transformation process. Kim *et al.*[23] and Matsukata *et al.*[24] confirmed that the dry gel conversion technique is useful for synthesizing various types of zeolite topologies, such as ANA, FER, MFI, MOR and CHA. In these syntheses the starting gel is never in direct contact with the aqueous liquid phase, but the vapor generated at the synthesis temperature, with or without the template, is the phase in contact with the amorphous solid gel. Although an excess of water was not essential for the zeolite synthesis, in some cases it promotes the

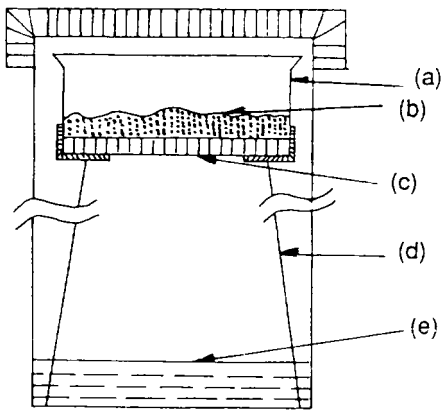

Fig. 3 Schematic illustration of the autoclave used in the zeolite synthesis by the VPT method: (a) container; (b) amorphous gels; (c) porous sieve plate; (d) stainless steel support; (e) solution phase. Reprinted with permission from reference 22.

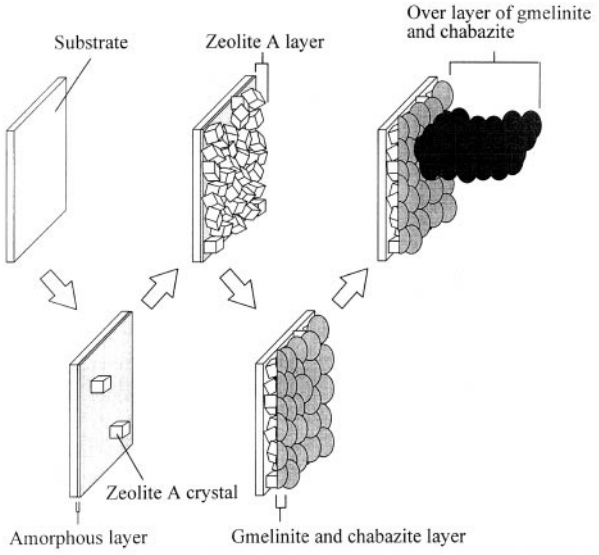

Fig. 4 Proposed mechanism for the formation of zeolite A membranes. Reprinted with permission from reference 29.

crystallization. It is interesting to note that in this type of syntheses, the dry gel can be fully converted to zeolite by selecting appropriate preparation conditions.

Matsukata and coworkers[25] were able to prepare high-silica beta zeolite, with higher SiO_2/Al_2O_3 ratios than those achieved by the conventional hydrothermal synthesis method, by the dry gel conversion treatment. In this case, a gel obtained by mixing aluminium sulfate, NaOH, tetraethylammonium hydroxide (TEAOH, the structure-directing agent) and colloidal silica was placed in a special autoclave similar to that shown in Fig. 3, with just water in the bottom. The kinetics of the crystallization depends on the SiO_2/Al_2O_3 ratio. For the highest aluminium content, changes in the crystallinity from 0 to 100% could be achieved in 30 min. The composition of the final crystalline phase was the same as in the starting gel, without the presence of amorphous phases. Interesting points are the uniformity of particle sizes with values around 60 nm and the requirement of water to obtain a crystalline product. This synthesis method has been successfully applied to prepare unsupported zeolitic membranes by Dong *et al.*[26] or alumina-supported zeolites by Matsukata *et al.*[27]

Although the gel includes, in this case, a third component (B_2O_3), Dong *et al.*[28] have shown that the vapor-phase transport method is useful also for synthesizing zeolite B-Al-ZSM-5 from boron–aluminium–silicon porous glasses with an ethylamine–water mixture as the vapor source. Analogously to the other works relating to this synthesis method, several experimental features, such as *e.g.* the similarity between the zeolite and gel compositions, have led the authors to postulate a heterogeneous crystallization mechanism.

Recently, Yamazaki and Tsutsumi[29] studied the synthesis of zeolite A membranes using a plate heater. This device allows one to distinguish between whether the membrane is produced on the surface of the substrate available for the growth of the zeolite film, or it is formed by accumulation of zeolite crystals arising from the liquid phase. The authors used a static method in which the source of silica and alumina, a liquid or an amorphous hydrogel, was placed in a PTFE vessel inside an autoclave and cooled by water circulation in order to prevent heating far from the plate heater. To avoid corrosion by alkaline components the plate heater was coated with PTFE, which also acts as substrate for the membrane synthesis. According to the results, the crystallization mechanism can be schematically described by Fig. 4, where an amorphous phase layer is generated on the substrate before the crystalline membrane covers the plate heater. The authors suggested that the formation of zeolite A nuclei takes place within the amorphous layer in which a high nucleation rate is present. At longer synthesis times, the subsequent growth of gmelinite and chabazite phases is observed.

2.2 Crystallization of pure silica zeolites

Davis and coworkers have made remarkable contributions to elucidate the role of the structure-directing agents in the synthesis of pure silica zeolites.[30,31] According to these authors, the addition of organic molecules such as amines and alkylammonium ions to zeolite synthesis gels can affect the rate at which a particular material is formed or can make accessible new structures or framework chemical compositions. Thus, while the synthesis of zeolite ZSM-5 can be achieved with a wide variety of framework silicon-to-aluminium ratios through numerous synthetic routes, both with and without organic species, pure silica ZSM-5 (silicalite-1) has been never synthesized in the absence of an organic structure-directing agent. In the as-synthesized silicalite-1, the TPA^+ cations are tightly coupled at the channel intersections with the propyl chains extending into both the linear and sinusoidal channels. The structure-directing agent can be removed only by calcination, suggesting that it is incorporated into the aluminosilicate or silicate structure during the process of crystal growth. Davis and coworkers used intramolecular cross-polarization (CP) ^1H–^{29}Si in conjunction with magic angle spinning (MAS) in solid state NMR to probe the interactions between the TPA^+ cations and the silicalite species that ultimately form the zeolite framework. Using fumed silica as the silicate source, the transformation of the starting gel into the zeolite was followed by means of this technique, leading to the spectra shown in Fig. 5. Although the atomic ordering characteristics of silicalite-1 were evident by both XRD and IR spectroscopy after the mixture was subjected to the synthesis conditions for two days, the amorphous solid obtained by heating just for one day showed cross-polarization between the TPA protons and

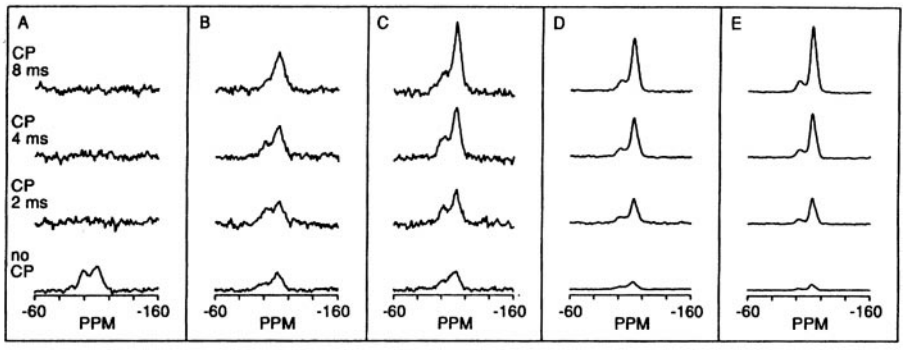

Fig. 5 ^{29}Si MAS NMR and ^1H–^{29}Si CP MAS NMR spectra of freeze-dried samples recorded during the TPA-mediated synthesis of silicalite-1: (a) unheated gel; (b) heated 1 day; (c) heated 2 days; (d) heated 3 days; (e) heated 10 days. Reprinted with permission from reference 30.

the silicon atoms. This feature was not detected in the unheated gel, which suggests that the TPA molecules and the silicate species were not in close proximity in the starting gel, although a very small proportion of TPA was incorporated in the solid silicate. Upon heating, the structure of the synthesis mixture undergoes dramatic transformations, showing a substantial modification at molecular level with TPA protons within the van der Waals distance of the silicon atoms in the amorphous silica gel. With further heating, XRD and IR spectroscopy identify crystalline silicalite-1, and the tight coupling of the TPA molecules within the fully formed channel intersections of the zeolite significantly enhanced the efficiency of ^{1}H–^{29}Si cross-polarization.

These observations are consistent with the mechanism proposed by Burkett and Davis[30] of structure direction by TPA in the synthesis of silicalite-1. The TPA cations interact with the silicate species and organize them into structures that are ultimately incorporated into the channel intersections of the zeolite product, as schematically depicted in Fig. 6. It thus appears that the TPA molecules are bonded to complex silicate structures through non-covalent intermolecular interactions prior to the appearance of long-range crystalline order. Therefore, self-assembled structures composed of TPA and silicate that may resemble the channel intersections of the product appear to be involved in the synthesis of silicalite-1.

Thompson and coworkers[32] have studied the use of seed crystals in the synthesis of silicalite-1 (secondary nucleation). Seed crystals added to a crystallization system should compete for nutrient material with any new nuclei that are formed. The greater the amount of seed crystal surface, the more successful the seed crystals should be in this competition. It was observed that the surface of Na^{+}-silicalite-1 seed crystals catalyzed the nucleation of new crystals, reducing the crystallization time with increased seeding levels. The authors postulated the existence of initial-bred nuclei on the surface of the seed crystals. Some of them are dislodged from the surface during the gel preparation, becoming nuclei in solution, while others remain on the seed crystals. A unique feature of the ammonium-based system was that the gel phase became very viscous (solid-like) after about 30 min at the synthesis temperature, so that the growing crystals were somewhat immobilized in the gel phase thereafter. The lack of settling of the product crystals and the quite uniform crystal size obtained in the unseeded syntheses suggested that nucleation occurred as spontaneous events before the solution became thick and the crystallization process had proceeded to completion.

The synthesis of pure silica zeolite Beta has been achieved by Corma and coworkers,[33] using TEA as template and fluoride ions at near neutral pH. Recently, Serrano, van Grieken and coworkers[34] concluded that the mechanism of crystallization in this type of synthesis is based on solid–solid transformations. As is shown in Fig. 7, the solid yield remains almost constant during the whole crystallization process and close to 27% of the mass of the starting gel, which corresponds to a 100% solid

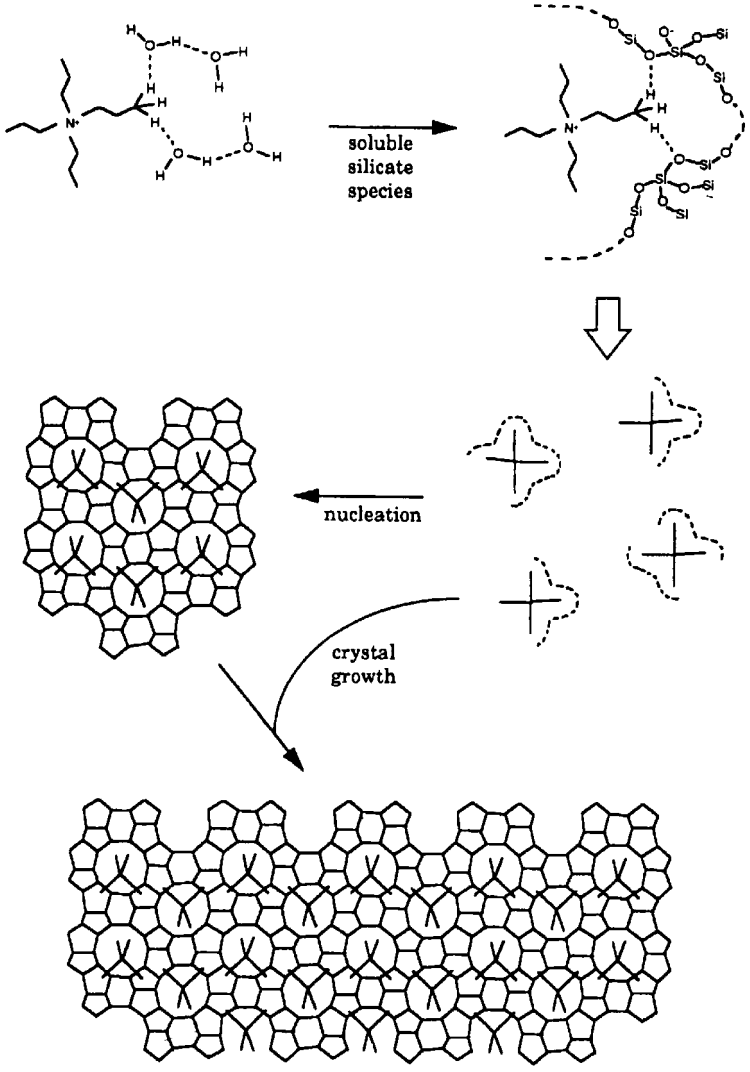

Fig. 6 Proposed mechanism of structure direction and crystal growth involving inorganic–organic composite species in the TPA-mediated synthesis of silicalite-1. Reprinted with permission from reference 30.

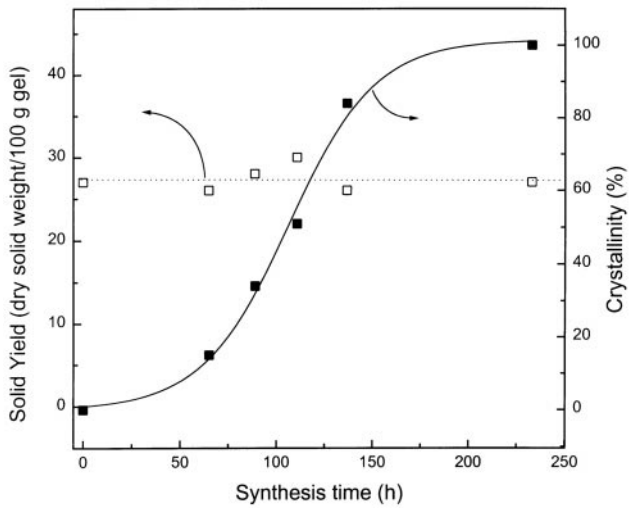

Fig. 7 Evolution of solid yield and crystallinity with synthesis time during the crystallization of pure silica zeolite Beta by the fluoride route. Reprinted with permission from reference 34.

yield on a silica basis. The first crystalline entities detected in the system, with sizes around 7 μm, grow directly from the amorphous solid phase through a process of aggregation and densification of primary units (10–30 nm) present in the gel phase (see Fig. 8(a) and (b)). In this case, the solid–solid transformations are probably favoured by the low solubility of the silica species in the fluoride medium at neutral pH.

2.3 Crystallization of titanium-containing zeolites

The research group in which we have been involved in from the early 1990s has focused attention on the synthesis of Ti-containing molecular sieves from wetness impregnated SiO_2–TiO_2 xerogels.[35–38] The procedure consists in the transformation of the SiO_2–TiO_2 xerogel into TS-1, a titanosilicate with MFI topology, by wetness impregnation with a TPAOH solution and subsequent heating to the synthesis temperature. The SiO_2–TiO_2 cogels, used as raw materials, were prepared through a two-step sol–gel route:[35] acid hydrolysis of the Si and Ti precursors (to avoid TiO_2 precipitation) followed by addition of a base to accelerate the condensation of the species in solution to yield a solid cogel. This solid is finally transformed with the appropriate structure-directing agent into the zeolite by autoclave treatment. The raw SiO_2–TiO_2 solids exhibit the Ti atoms dispersed in a polymeric SiO_2 network through the formation of Si–O–Ti bonds prior to the zeolite synthesis. The properties of the TS-1 samples depend on the method used to prepare the cogel. From the results obtained, the mechanism depicted in Fig. 9 has been proposed:

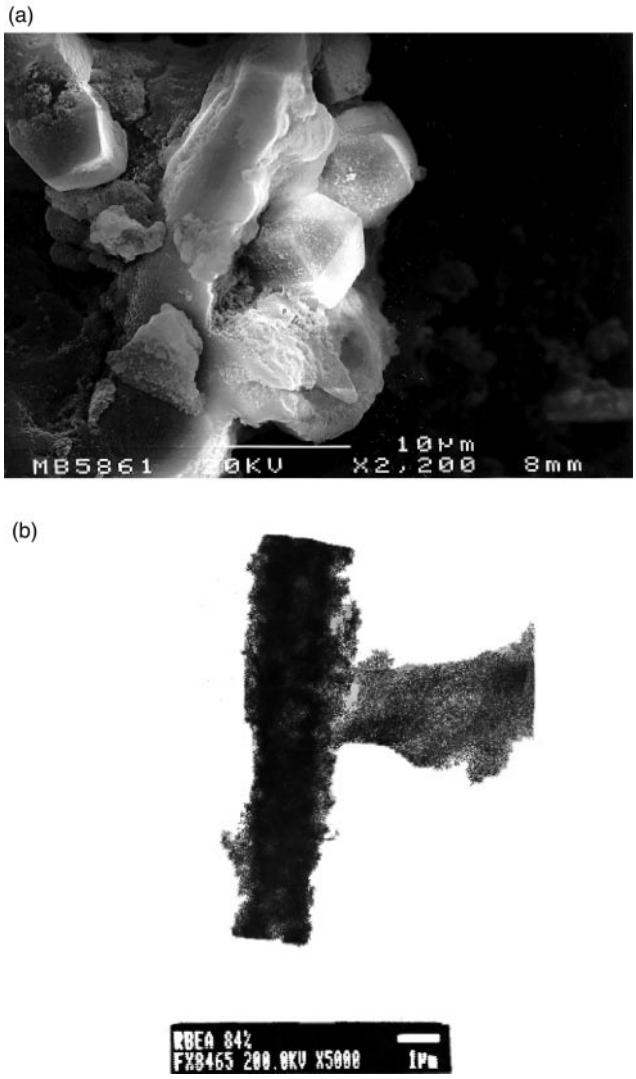

Fig. 8 Electron micrographs of partially crystalline samples during the crystallization of pure silica zeolite Beta by the fluoride route: (a) SEM image; (b) TEM image. Reprinted with permission from reference 34.

(1) The polymeric SiO_2–TiO_2 xerogel (Ti = 3.23%) is converted into a particulate material formed by amorphous primary particles with sizes around 50 nm. The cogel loses most of the macroporosity due to the tight packing of the primary particles. Simultaneously, a small portion of the starting material is dissolved, increasing the SiO_2 content of the solid (Ti = 1.94%).

(2) The primary particles in the cogel undergo an aggregation process, leading to the formation of secondary particles. The latter become independent from the cogel once they reach a

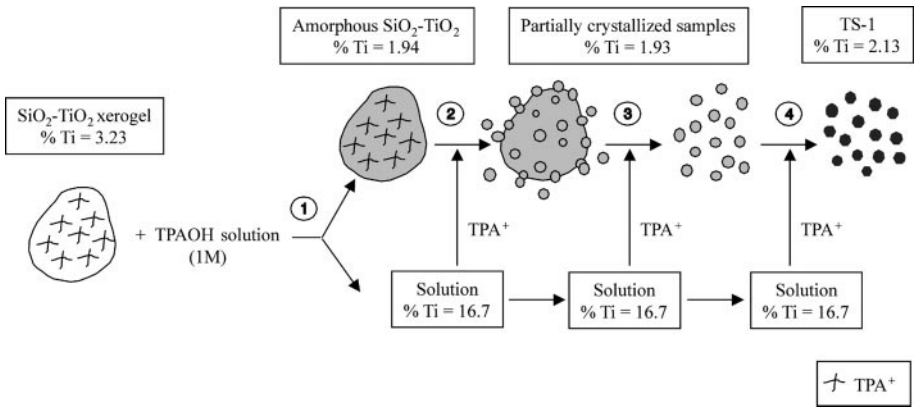

Fig. 9 Proposed mechanism for the crystallization of TS-1 zeolite from amorphous SiO_2–TiO_2 xerogels (%Ti = [Ti/(Si + Ti)] × 100). Redrawn with permission from reference 37.

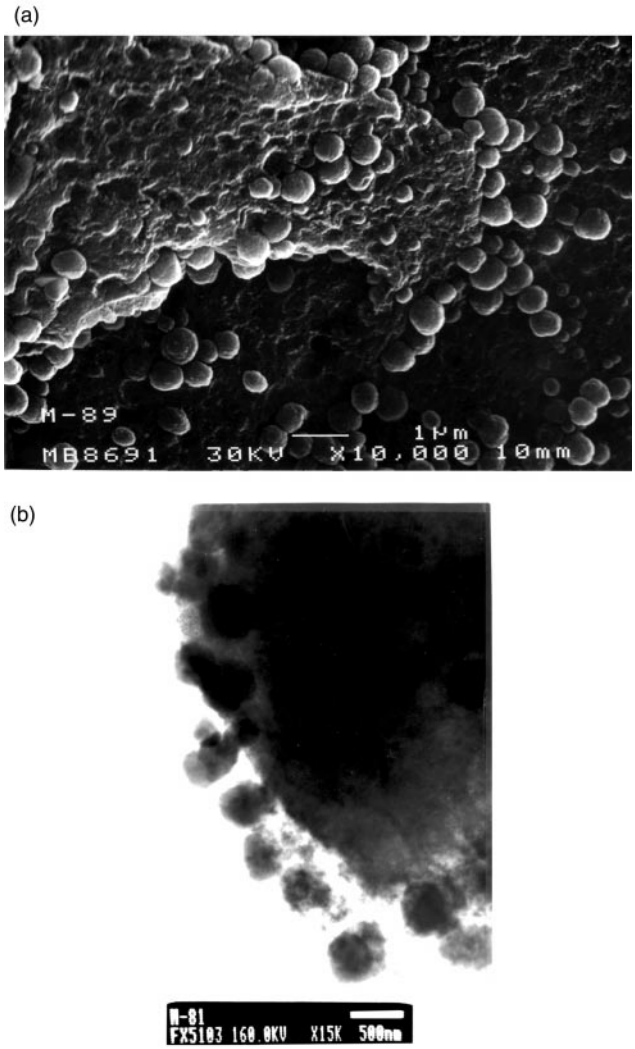

Fig. 10 Electron images of partially crystalline samples obtained in the synthesis of zeolite TS-1 from amorphous SiO_2–TiO_2 xerogels: (a) SEM image; (b) TEM image. Reproduced with permission from reference 37.

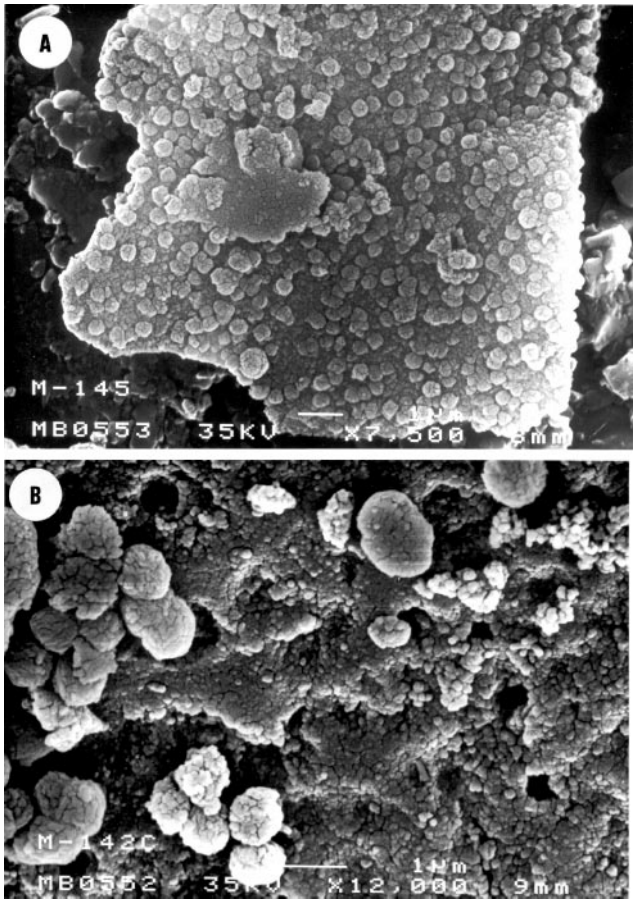

Fig. 11 SEM images of samples obtained in the crystallization of zeolite TS-2 from SiO_2–TiO_2 xerogels for different synthesis times: (a) heated 5 h, 0% crystallinity; (b) heated 12 h, 47% crystallinity. Reproduced with permission from reference 39.

critical diameter around 0.5 μm (see Fig. 10(a)). Moreover, a close inspection of the samples by TEM indicate that the primary units are not completely densified particles, but consist of aggregates of smaller nanoparticles (see Fig. 10(b)). At this point, the first signs of long-range order begin to be detected by X-ray diffraction.

(3) The secondary particles are gradually transformed into TS-1 crystals through a densification–zeolitization process. Accordingly, the final size and shape of the crystals are closely related to those of the initially amorphous secondary particles. In this type of synthesis, there is not a true crystal growth since the zeolite crystals are formed by zeolitization of the amorphous secondary particles as a whole.

A synthesis procedure analogous to that above for TS-1 was further developed for the preparation of zeolite TS-2, a crystalline Ti-containing material with MEL topology.[38,39] In this case, tetrabutylammonium hydroxide (TBAOH) was used as the structure-directing agent. The authors conclude that the crystallization mechanism is very similar to that of TS-1, being governed mainly by solid–solid transformations. Thus, the yield and the Ti content of the solid phases remain, also in this case, almost constant during the crystallization. Likewise, as shown in Fig. 11, pseudocrystalline secondary particles are formed by aggregation of primary units. TEM images show that both primary and secondary particles are really formed by smaller units with sizes in the nanometer range. It is interesting to point out that in the TS-2 synthesis the secondary particles remain in contact with the amorphous particulate solid as they are crystallized, which leads to a high degree of intergrowth and agglomeration of the final zeolite crystals and particles.

Gabelica and coworkers[40] reported an interesting contribution relating to the presence of heterogeneous phenomena in zeolite crystallization, based on the synthesis of titanosilicates by the *in situ* seeding method. The synthesis of TS-1 was studied using $TiCl_4$, solid SiO_2 and tetrapropylammonium bromide in alkali-free methylamine media, with different types of seeding. In addition to a conventional seeding with silicalite-1 crystals, a preheated silicate gel was also added in some cases to the synthesis mixture prior to the Ti source addition (*in situ* seeding). It is interesting to note that, while the conventional seeding method led to silicalite-1 with most of the titanium remaining in the unreacted gel, the *in situ* seeding alternative accelerated the crystallization of TS-1 and promoted the incorporation of Ti in framework positions. This result strongly suggests that the added silicate phase is directly involved in the crystallization. The preheating time of the precursor silicate gel turned out to be an important factor since too short preheating led to slow TS-1 crystallization while too long resulted in the formation of silicalite-1 crystals.

In the preparation of zeolites from wetness impregnated xerogels, a partial or complete dissolution of the starting gel has been observed in some instances during the first steps of the crystallization. Thus, when Al-TS-1 is synthesized from SiO_2–TiO_2–Al_2O_3 xerogels most of the Al species remain in the solid state while a preferential dissolution of both Ti- and Si-containing species takes place.[41] Simultaneously, the polymeric solid is converted into a particulate amorphous material formed by a tight packing of primary units. Aggregation of the latter leads to secondary particles that become independent

from the cogel once they reach a critical size of 0.5 μm. In the final step, a slow incorporation of species from the solution occurs accompanied with a densification of the secondary particles and their transformation into zeolite crystals. On the other hand, a surprising result has been observed when Al–Ti Beta zeolite is synthesized using the wetness impregnation method.[42] In this case, the complete dissolution of the starting xerogel takes place, followed by the formation of an amorphous gelatinous solid phase consisting of a tight packing of primary particles with sizes around 10 nm. This amorphous phase is rich in aluminium species which limits and hinders the Ti incorporation. The crystallization of zeolite Beta takes place mainly by reorganization of the primary particles present in the amorphous gelatinous phase through an aggregation–densification–zeolitization process. In the last stage of the crystallization, a slow incorporation of silicon and titanium species from the solution contributes to the formation of the final zeolite Beta crystals.

3. Zeolite crystallizations from clear solutions

In these systems, the starting clear solutions are usually obtained by the hydrolysis of monomeric silica species, although in some cases they are derived from the depolymerization of polymeric silica sources. The absence of macroscopic solid phases in the starting mixture allows *in situ* spectroscopic techniques to be used for monitoring the crystallization. Thus, light-scattering analyses have been recently applied in a number of works.

Since the raw clear solutions used in these systems are free of amorphous solid phases, it was initially thought that the zeolite crystallization proceeds directly from the solution phase. However, the formation of an X-ray amorphous phase with a gelatinous aspect has been often observed prior to the detection of the first zeolite crystals, raising a number of questions about its role during the crystallization. Works relating to the crystallization mechanism of these type of synthesis are described below, being classified according to the chemical composition of the zeolite obtained.

3.1. Crystallization of aluminium-containing zeolites

Compared to the pure silica zeolite synthesis, the crystallization mechanism of zeolites from clear solutions in the presence of Al sources has not been studied as deeply. Probably, the reason is that the simplest system has been usually the preferred choice for these mechanistic investigations. The presence of Al may modify the crystallization pathway as the Al species are expected to participate in both nucleation and crystal growth steps. However, at the same time, the Al species may act as very useful probes for the understanding of the crystallization mechanism, since the evolution of their content, coordination and environment may be followed by a number of techniques.

The nucleation step in the crystallization of zeolite NaA from clear solutions with initial seeding has been investigated by Gora and Thompson.[43] It was observed that the addition of small seed crystals, with sizes in the range 1–3 μm, to a clear solution synthesis batch did not promote the nucleation. However, initial seeding with much larger zeolite NaA crystals (40 μm size) led to the formation of a second zeolite crystal population. Small particulates, formed by residual aluminosilicate material located on the external surface of the large zeolite crystals, were proposed to act as nuclei of zeolite NaA.

Davis and coworkers[44] have studied the synthesis of zeolite L from clear solutions by high-resolution transmission electron microscopy (HRTEM). Zeolite L is a material with a one-dimensional large-pore system parallel to the *c*-axis. The unit cell contains 36 tetrahedrally coordinated T atoms and has the composition $K_9[Al_9Si_{27}O_{72}]\cdot 21H_2O$. The syntheses of zeolite L were carried out at 175 °C in the absence of any organic compound. After 1 h of heating, the clear starting solution was transformed into a gelatinous gel with a Si/Al/K ratio close to that of the final zeolite product. The solid yield remained almost constant during the crystallization. HRTEM images showed that the zeolite L crystals are actually clusters of aligned and connected nanometer domains, which present a direct correlation in size with the units observed in the gelatinous gel (around 20 nm size). According to these results, the authors propose that in this system the zeolite crystallization takes place from the amorphous gel precursor through local rearrangements of the former. As the zeolite grows, the solid shrinks as a consequence of the higher density of the zeolite compared to the precursor gel. This crystal growth is proposed to take place by propagation of isolated nucleation events through the gel network.

Regev *et al.*[45] have studied the crystallization of zeolite ZSM-5 from clear solutions by means of cryo-TEM, and small- and wide-angle X-ray scattering measurements (SAXS and WAXS, respectively). The starting reaction mixture was prepared using polymeric silicic acid, aluminium metal powder, NaOH and TPAOH. Cryo-TEM images of this precursor solution showed the presence of globular structural units with sizes around 5 nm, that gave an amorphous pattern when examined by WAXS. These globular units were not observed in solutions with pH below 11.6, which indicates that strong basicity is necessary for their formation. After 2 h of heating at 150 °C, aggregation of the globular units into cylindrical bodies was detected by TEM. This event did not take place in solutions free of TPAOH. The cylindrical bodies are proposed to be formed by aggregation of 5 globular units, having a diameter of 8 nm and a length of 22 nm after 1 h of synthesis. Likewise, it is proposed that each globular unit is composed of several tetrapods, which are assumed to be crystalline. Accordingly, the amorphous WAXS pattern corresponding to these units is explained by the small size of the crystalline entities in the globular units.

The synthesis and crystallization mechanism of zeolite ZSM-5 with crystal sizes in the range 50–100 nm has been investigated by van Grieken *et al.*[46] starting from clear solutions, prepared by hydrolysis of tetraethylorthosilicate and aluminium isopropoxide with aqueous TPAOH. During the first hours of synthesis the formation of an amorphous solid gel phase is detected, consisting of particles with sizes below 10 nm. These primary units undergo an aggregation process to yield secondary particles with sizes around 20 nm. While the primary units appear X-ray amorphous, some diffractions are detected in the secondary particles during the TEM measurements. The aggregation and zeolitization of the secondary particles lead to the formation of the final zeolite crystals with sizes in the range 50–100 nm. ^{27}Al MAS NMR spectra of the samples obtained at different synthesis times show that in all cases the Al species present tetrahedral coordination, regardless of the sample crystallinity. N_2 adsorption measurements at 77 K indicate that the amorphous gel phase is a solid with a high surface area (around 700 $m^2\,g^{-1}$) and a significant presence of microporosity. The crystallization mechanism of zeolite ZSM-5 proposed by the authors considers that the zeolite crystals are formed by reorganization and aggregation of the nanoparticles present in the amorphous gel phase, formed at the beginning of the synthesis. However, a contribution of a solution-mediated crystallization is also postulated to explain the appearance of a second population of large crystals at the end of the synthesis, which occurs simultaneously with a sudden increase in the solid yield.

3.2. Crystallization of pure silica zeolites

The synthesis of zeolites in the absence of aluminium has been commonly selected in recent years as a model system for studying the crystallization mechanism due to its simplicity. Silicalite-1, the all silica member of the MFI topology, is the

material most widely investigated, since this material can be easily synthesized in the presence of TPA^+ species at relatively low temperatures and short synthesis times.

One of the pioneering studies on the use of light-scattering techniques in the investigation of zeolite crystallizations is the work of Twomey *et al.*[47] Two different analysis techniques were used: dynamic light scattering (DLS), also known as quasi-elastic light scattering (QELS), and static light scattering (SLS). These measurements provide essential information about the size, in the nanometer range, of the particles present during the zeolite crystallization. The authors studied the nucleation and growth of silicalite-1 from clear solutions prepared from silicic acid, NaOH, TPAOH and water. They observed a continuous and almost linear increase of the particle size from 20 nm up to 150 nm with synthesis time. Extrapolation of the growth curve to zero particle size evidences that an initial induction time exists in this system, being interpreted as the time necessary for the formation of viable nuclei from the soluble silicates present in the homogeneous solution. The length of this induction period was significantly shortened by aging of the clear solution at room temperature, indicating that the raw solution is not dormant, but viable nuclei are being generated even at low temperature. From experiments carried out at different temperatures, it was possible to determine the apparent activation energy of both nucleation and crystal growth steps: 94 and 96 kJ mol^{-1}, respectively. According to the authors, these high values indicate the strong effect of the temperature on the silicalite-1 synthesis, and suggest that the rate-controlling step is not a diffusional process, but chemical interactions between silicate species.

Schoeman and coworkers have investigated in a series of papers[48–54] the early stages in the crystallization of silicalite-1 from clear solutions, prepared by hydrolysis of TEOS with TPAOH. Under the conditions used, the silicalite-1 obtained is formed by crystals with sizes below 100 nm, hence they can be considered as discrete colloidal particles. At short times, the product of the synthesis is formed by particles of lower size that appear to be amorphous when analyzed by X-ray diffraction.

The initial stages of the crystallization were investigated by both DLS and cryo-TEM.[50,51] As shown in Fig. 12, a linear growth of the particle size from around 10 nm takes place with synthesis time. Surprisingly, a second population of particles, with sizes around 3–5 nm, is also detected during the whole crystallization, denoted as subcolloidal particles. Accordingly, after 10 h of synthesis the particle size distribution is bimodal. While the size of the largest particles increases continuously with time, becoming the final silicalite-1 crystals, the size of the subcolloidal particles does not show a clear trend with time, with a maximum being observed at 10 h of synthesis.

Another significant result derived by this research group was the fact that the formation of the subcolloidal particles takes place even at room temperature previous to the hydrothermal crystallization.[52,53] The starting synthesis solution seems to be a completely clear and homogeneous liquid phase. However, when observed by cryo-TEM, the presence of subcolloidal particles with sizes around 3 nm is evidenced also in such raw clear solutions. In a further work, the subcolloidal silica particles were extracted from the precursor solution, being obtained as a powder. The extracted solid was characterized by a number of techniques: Raman and DRIFT spectroscopies, N_2 adsorption and electron diffraction during TEM analysis. Raman spectra indicate the presence of TPA^+ cations entrapped in the silicate structure of the subcolloidal particles. It is proposed that the TPA^+ cations are incorporated within the silica particles at the same time as they are formed during polymerization of the silica species arising from TEOS hydrolysis. As shown in Fig. 13, the DRIFT spectra of the extracted solids present an absorption band at 560 cm^{-1}, usually assigned to highly distorted double six rings in the MFI zeolitic structure. Upon calcination of the extracted

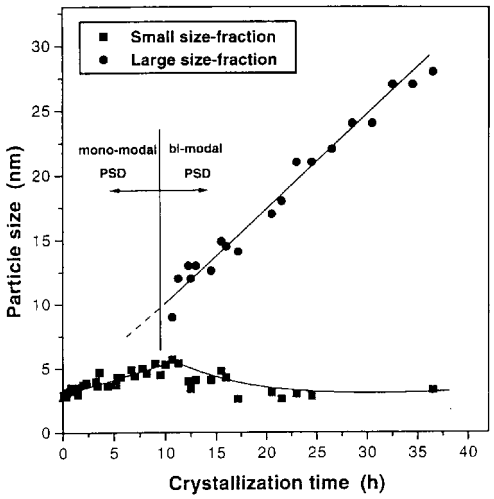

Fig. 12 Changes in the average particle size as a function of the crystallization time during the synthesis of silicalite-1 from clear solutions. Reprinted with permission from reference 50.

subcolloidal particles, this band almost disappears, which indicates that they are not as stable as the final silicalite-1 crystals.

According to Schoeman and coworkers, different alternatives can be proposed to explain the role of the subcolloidal particles in the silicalite-1 crystallization. The first is the direct participation of these particles in the whole synthesis mechanism as both nuclei and building blocks during the crystal growth step. The second alternative considers that these particles are simply a reservoir of nutrients for the growing crystals, *i.e.* the subcolloidal units undergo a progressive dissolution along the crystallization leading to soluble silica species, which are further incorporated into the zeolite crystals following a homogeneous process. Finally, a third possibility is that nucleation takes place on the subcolloidal particles, whereas the subsequent crystal growth proceeds by addition of monomeric species. Based on the extended Derjaguin–Landau and Verwey–Overbeek (DLVO) theories, applied to colloidal systems, Schoeman[54] concludes that it is unlikely that the silicalite-1 crystals grow *via* a particle–particle aggregation mechanism due to the presence of repulsion forces, although some aggregation may occur among the subcolloidal particles or between them and growing crystals.

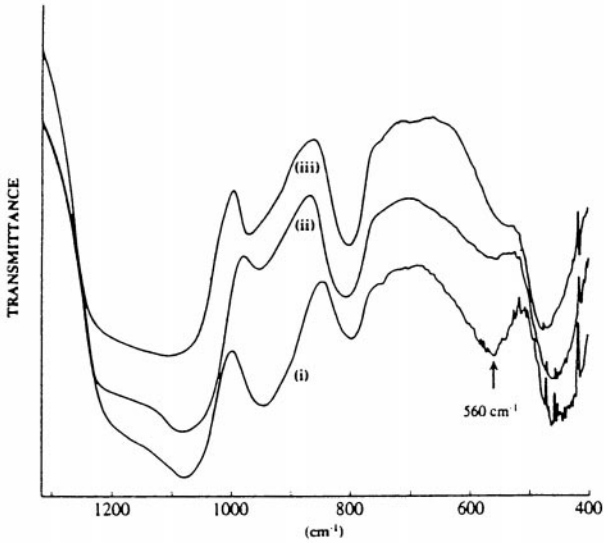

Fig. 13 Crystallization of silicalite-1 from clear solutions. DRIFT spectra of freeze dried powders: (i) sample containing subcolloidal silicate particles; (ii) this sample after calcination; (iii) sample of truly amorphous silica particles (Ludox SM). Reprinted with permission from reference 53.

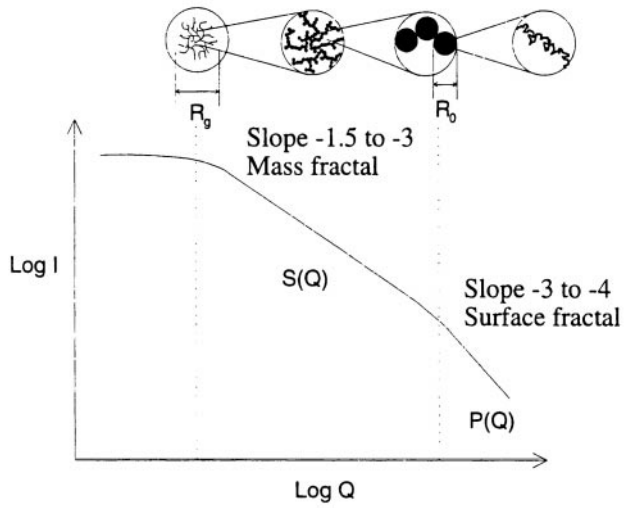

Fig. 14 Crystallization of silicalite-1 from clear solutions. Relationship between the X-ray scattering spectrum and the particle structure and size. R_g is the size of an aggregate with mass fractal properties, which is built up of primary particles of size R_0 with surface fractal properties. Reproduced with permission from reference 56.

The crystallization mechanism of silicalite-1 from clear solutions has been also investigated in detail by van Santen and coworkers in a series of papers[55–60] using both small- and wide-angle X-ray scattering measurements (SAXS and WAXS, respectively). Fig. 14 shows the relationship between the scattering spectrum and the particles present in the synthesis gel which are responsible for that scattering. From these *in situ* measurements, the authors identify the presence of particles with sizes around 3 nm during the whole silicalite-1 crystallization process. Moreover, it is concluded that the 3 nm size particles tend to form mass fractal aggregates yielding larger particles, with diameters in the range 7–10 nm. The formation of these colloidal aggregates seems to be dependent on the basicity of the synthesis medium.[56] At relatively low alkalinities (Si/OH $<$ 2.65), the formation of aggregates is observed previously to the onset of crystallization. However, under more basic conditions, no aggregates are detected.

To explain these results, the authors have proposed different possible crystallization mechanisms. Initially, it was suggested that the formation of the silicalite-1 crystals from the subcolloidal particles takes place by a combination of aggregation–densification steps, as illustrated in Fig. 15.[55] However, in further papers[56,57] the possibility of a homogeneous mechanism is also postulated, which considers the colloidal aggregates to act simply as a source of amorphous silica, being transformed into subcolloidal particles and/or silicate species as the crystallization progresses. This mechanism should be favoured at higher alkalinity, as a consequence of the higher solubility of the silica.

In a recent work from van Santen and coworkers,[58] the crystallization of silicalite-1 has been investigated using a combination of X-ray scattering techniques, as well as by means of electron microscopy. The simultaneous use of wide-, small-, and ultra-small X-ray scattering (WAXS, SAXS and USAXS, respectively) has allowed these authors to study the crystallization events on a continuous range of length scales, from 0.17 up to 6000 nm, covering all the particle populations that may appear during the crystallization. Moreover, time-resolved experiments have been performed through the use of high-brilliance synchrotron radiation. The results obtained confirm the presence of two types of precursor particles: primary units with 2.8 nm size and aggregates with diameters around 10 nm. As shown in Fig. 16, both subcolloidal particles and aggregates are observed prior to the detection of the first signs of crystallinity, which is indicated by the appearance of

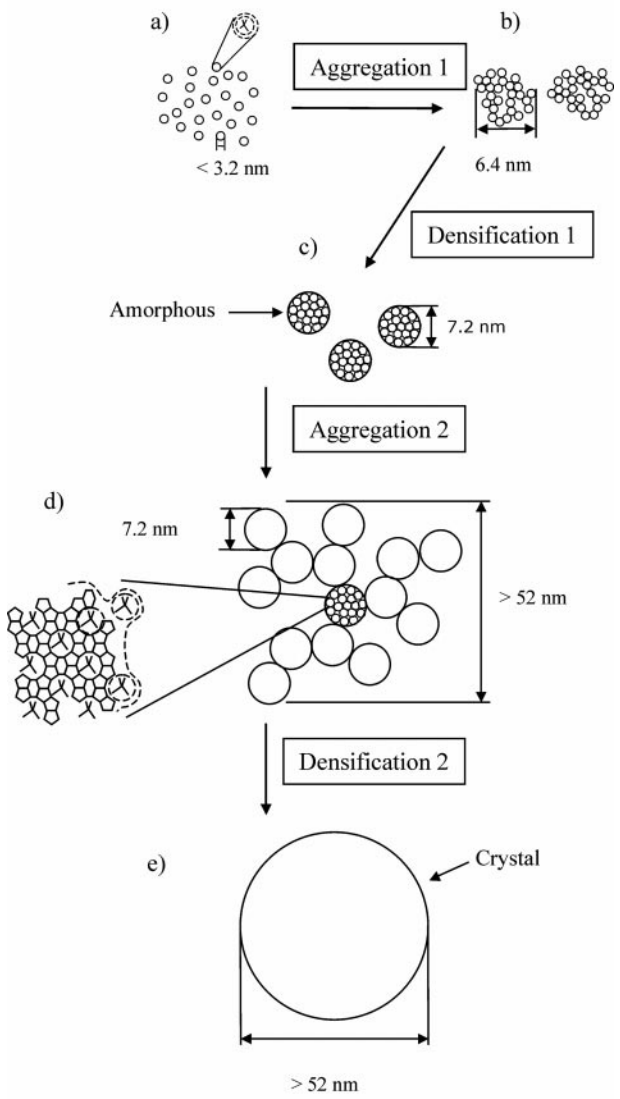

Fig. 15 Proposed mechanism for the crystallization of silicalite-1 from clear solutions: (a) silicate/TPA clusters in solution; (b) primary fractal aggregates formed from the silicate/TPA clusters; (c) densification of these primary fractal aggregates; (d) combination of the densified aggregates into a secondary fractal structure and crystallization; (e) densification of the secondary aggregates and crystal growth. Redrawn with permission from reference 55.

Bragg reflections. A sharp decrease in the concentration of the aggregates occurs simultaneously with the onset of crystallization, whereas the population of subcolloidal particles starts decreasing somewhat later. It is also observed that, while the formation of the 2.8 nm primary units is independent of the alkalinity, the concentration of aggregates is strongly affected by this parameter, no aggregates being detected at high alkalinity (Fig. 16(a), Si/OH = 2.42).

Based on these results, the authors propose a mechanism for the silicalite-1 synthesis which considers that both the subcolloidal particles and aggregates are directly involved in the crystallization. The primary units are formed by dissolution of the silicic acid in the TPAOH solution. These subcolloidal particles are assumed to be composite organic–inorganic units which show a degree of ordering, but are not still completely organized in a crystalline lattice. The second population of particles, with sizes around 10 nm, is formed by aggregation of the primary units. The concentration of aggregates depends on the alkalinity of the synthesis medium and it shows also a strong correlation with the number of crystals finally formed, *i.e.* with the nucleation rate. Accordingly, it is proposed that the formation of the aggregates is an essential step in the

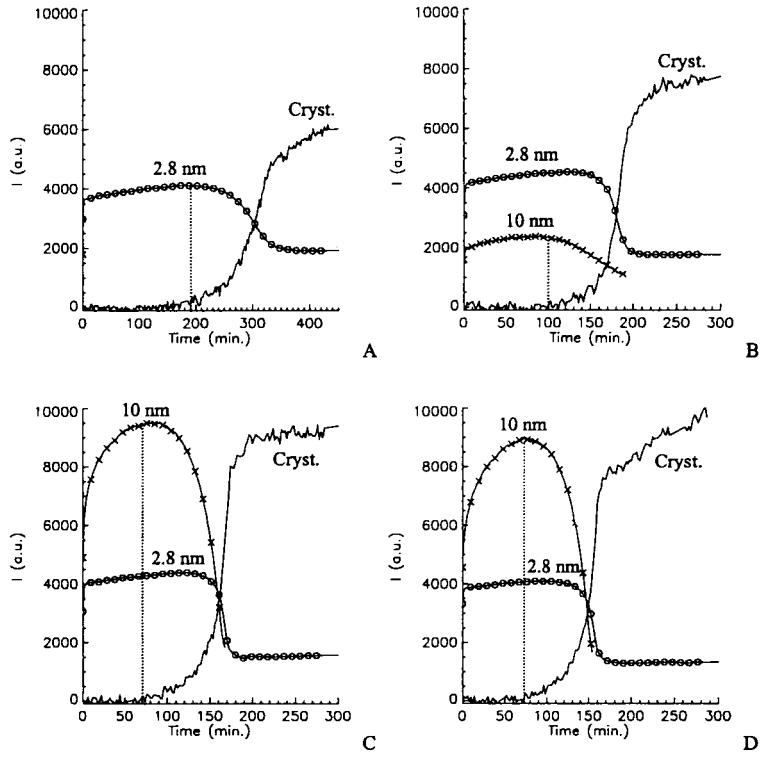

Fig. 16 Crystallization of silicalite-1 from clear solutions. Time-dependent scattering intensity at fixed angles, corresponding with a *d* spacing of 2.8 nm (primary units) and 10 nm (aggregates), together with the area of the Bragg reflections from the formed silicalite-1 crystals, for synthesis mixtures with different Si/OH ratios: (a) 2.42; (b) 2.57; (c) 2.72; (d) 3.02. Reprinted with permission from reference 58.

nucleation process. Likewise, it is concluded that the crystal growth step proceeds by incorporation of the primary units, with 2.8 nm size, at the crystal surface. From experiments carried out at different temperatures, an apparent activation energy of 83 kJ mol^{-1} is obtained for the crystal growth step. This high value indicates that a diffusion-controlled growth is not taking place, whereas it agrees well with the assumption that the crystal growth rate-limiting step is the addition of the subcolloidal particles at the crystal surface. In a recent work of van Santen, Davis and coworkers,[59] this mechanism has been concluded to be also valid when changing the organic molecule used as structure-directing agent. Experiments were carried out by substituting TPAOH by hexamethylenebis(tripropylammonium) dihydroxide (dimer of the TPA^+ cation), and hexamethylene-*N*,*N*′-bis(tripropylammonium)-*N*″,*N*″-dipropylammonium trihydroxide (trimer of TPA^+). Both primary units with 2.8 nm diameter and aggregates with sizes in the range 10–15 nm have been also detected in the silicalite-1 synthesis with these templates. The results obtained in this work show that the template used does not influence the size of the primary units, although it has a pronounced effect on the crystal growth step, which in turn determines the final size and morphology of the crystals.

This crystallization mechanism has been extended for the synthesis of other pure silica zeolites different from silicalite-1. Thus, the crystallization of the all-silica BEA and MTW zeolite structures has been investigated using the same template (trimethylenebis(*N*-benzyl-*N*-methylpiperidinium)) and silica source (TEOS).[60] At low template concentration the MTW zeolite is the main product of the crystallization, whereas the BEA structure is preferentially formed from systems with a high template content. In both cases, the raw synthesis mixture is a clear solution at room temperature, but it becomes cloudy when the synthesis temperature (150–160 °C) is reached, which indicates the formation of a heterogeneous gel phase in the early stages of the crystallization. SAXS and USAXS measurements showed the presence of X-ray amorphous nano-sized primary units in both systems. For the BEA structure, these primary units show a size of 2.6 nm, whereas in the MTW synthesis particles with a diameter of 1.5 nm are detected. According to the authors, these results suggest that a general mechanism may account for the organic-mediated crystallization of different high-silica zeolite structures, based on nanometer primary units. The exact size of these primary particles depends on the zeolite topology being formed.

The crystallization mechanism of silicalite-1 from homogeneous solutions containing TPA as template has been also investigated by White and coworkers[61,62] using different *in situ* and *ex situ* techniques. These authors classify the zeolite synthesis in two categories, which depends on the absence (homogeneous crystallization) or the formation (heterogeneous crystallization) of a gelatinous intermediate phase, previous to the detection of the first crystalline material. Moreover, in some syntheses the formation of a dense gel is observed after mixing the sodium silicate used as silica source and the TPABr solutions. From experiments carried out varying the composition of the synthesis mixture, the authors propose the crystallization field shown in Fig. 17. In agreement with this picture, homogenous crystallization occurs only at low concentrations of both silica and TPA. Upon increasing these concentrations, the silicalite-1 crystallization takes place by a heterogenous pathway, involving the formation of the gelatinous amorphous phase as an intermediate stage, over a wide range of compositions. Finally, at high concentration of both SiO_2 and TPA, gelation of the synthesis mixture is observed instead of zeolite crystallization. The authors then selected a composition corresponding to the homogenous crystallization region to be further studied in detail. From the SAXS pattern, the presence of particles with an average size around 9.4 nm was observed throughout the crystallization. When isolated from the synthesis mixture, these particles appear to be formed by X-ray amorphous material, whereas their characterization by FTIR indicates the presence of the bands at 550–560 cm^{-1}, typical of the MFI zeolite structure. Moreover, from small-angle neutron scattering measurements (SANS), it is concluded that TPA molecules are occluded

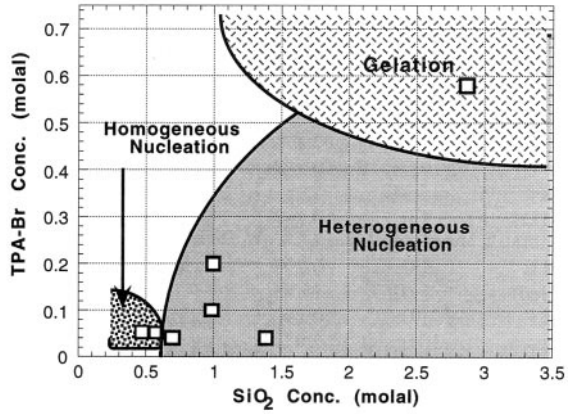

Fig. 17 Crystallization field for TPA-silicalite. Reprinted with permission from reference 62.

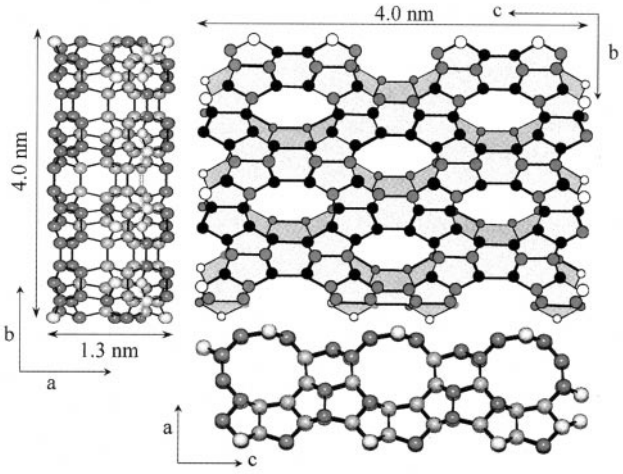

Fig. 18 Proposed structure and dimensions of a silicalite-1 nanoslab. Reprinted with permission from reference 63.

within these particles. Accordingly, it is suggested that the nanosized particles are the zeolite nuclei. In regards to the shape of these particles, the best fitting of the SAXS and SANS patterns is obtained when they are considered to be cylindrical entities. The initial size of these units, after just 2 h of synthesis, is estimated to be around 8 nm diameter and 14 nm length. After this period, the average diameter remains almost constant with the crystallization time, whereas the length of the cylinders increases steadily, which suggests that they grow by a sequential coaxial fusion of the cylindrical primary units. This picture is also confirmed from SEM images of the freeze-dried samples, which evidences that the aggregation of very small particles gives rise to large silicalite-1 crystals.

Based on the earlier results and conclusions, White and coworkers[62] proposed the following mechanism to explain the silicalite-1 crystallization. In the first step, the cylindrical primary nuclei are formed with the incorporation of TPA species. Subsequently, these units fuse coaxially to yield primary crystallites with an average diameter of 8.3 nm and an average length of 33 nm. Finally, a rapid crystal growth step takes place by aggregation of the primary crystallites to form ellipsoidal crystals in the micron range.

An interesting result is the fact that those authors observe a significant discrepancy between the diameter estimated for the cylindrical primary particles from SANS and SAXS patterns. They propose that these particles have an internal structure consisting of a core with an annular shell, where the radii of the cores are given by the SANS measurements, while the SAXS results yield the total radii corresponding to the cores with their shells. It is suggested that the cores are compact and present a well-organized MFI framework with encapsulated TPA cations, whereas the shells are formed by a highly defected structure with a high fluid content. This combination of perfectly crystalline cores and partially amorphous shells is also essential to explain the formation of the final crystals, as it is proposed that the ordering of the disordered shells of the primary crystallites accompanies their aggregation in the final crystallization stage.

The whole process of silicalite-1 crystallization from TPA-containing clear solutions has been studied by Jacobs, Martens and coworkers in a series of recently published papers.[63–66] In the first work,[63] the subcolloidal particles present in the starting synthesis mixture were isolated and characterized. TEOS was used as silica source, being hydrolysed by contacting with aqueous TPAOH. The solid material present in this macroscopically clear solution was extracted by a sequence of acidification, salting out, phase transfer into an organic solvent, and freeze drying. After these treatments, a white powder was obtained in a yield of 80% relative to the raw silica content. The low angle X-ray scattering pattern (XRS) of this solid is similar to that of the raw solution, which indicates that they are formed by the same entities. Characterization of this solid by TEM, atomic force microscopy (AFM), and ^{29}Si MAS NMR reveals it is formed by particles with sizes in the nanometer range. The best fitting of the Q^n distribution in the ^{29}Si MAS NMR spectra is obtained when these units are assumed to present slab geometry with dimensions of 4.0×1.3 nm. Although these nanoslabs are X-ray amorphous, the authors propose that they are crystalline units with the MFI topology corresponding to silicalite-1 (see Fig. 18). The absence of Bragg reflections is assigned to the small size of the nanoblocks. TG analyses of these particles show a weight loss of 6.6 wt% between 240 and 400 °C, assigned to the removal of TPA species. This weight loss accounts for 9 TPA molecules per nanoslab, which is in agreement with the 9 channel intersections present in the proposed slab model. From these results, the authors conclude that even in the starting synthesis solution, previous to the thermal crystallization, the MFI topology is already realized.

In a further work,[64] the early stages of the hydrolysis and polycondensation of TEOS was studied by means of ^{29}Si liquid NMR and *in-situ* infrared spectroscopy. These techniques allowed the different silicate polyanions present in the solution to be identified, and confirmed the existence of interactions between those species and TPA molecules. Fig. 19 illustrates the different species involved in the TPA-directed polycondensation of TEOS. It is proposed that one of the keys of the process is the hydrophobic surface created by the propyl chains of the TPA molecule. The different silicate polyanions identified (bicyclic pentamer, pentacyclic octamer, and tetracyclic undecamer) are organized and grow as a curved hydrophobic SiO_2 surface around the TPA molecules with the hydroxy groups pointing outward. During this process, a bifunctional interface with an outer hydrophilic and an inner hydrophobic surface is created. According to this model, the TPA molecules are proposed to be located preferably at the liquid–liquid interface in the raw emulsion. Moreover, the authors suggest that the structure direction by the template takes place simultaneously with TEOS hydrolysis. At room temperature, the polycondensation process ends with the formation of a species containing 33 Si atoms and one TPA molecule (trimer), which is considered to present the same framework connectivity as the bulk MFI zeolite. The dimensions of this trimer are estimated to be $1.3 \times 1.3 \times 1$ nm.

The formation of the nanoslabs from the trimers has been investigated with *in-situ* XRS and gel permeation chromatography (GPC).[65] The chromatograms corresponding to the raw clear solution used in the silicalite-1 synthesis exhibit several peaks with molecular weights that indicate they arise from the monomer, dimer, trimer, hexamer, nonamer and even heavier species, which are identified as aggregates of the trimer. Based

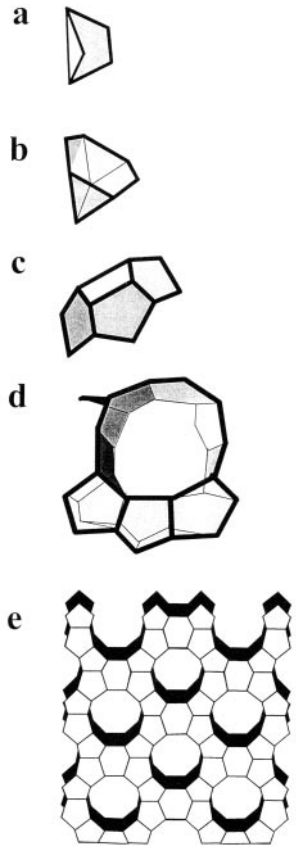

Fig. 19 Siliceous entities proposed to occur in the silicalite-1 crystallization from the TPAOH–TEOS system: (a) bicyclic pentamer; (b) pentacyclic octamer; (c) tetracyclic undecamer; (d) trimer; (e) nanoslab. Reprinted with permission from reference 65.

on these results, an aggregation mechanism of the trimers is proposed to explain the formation of the nanoslabs, which is depicted in Fig. 20. In a first step, three trimers are linked along the *c* axis to yield a nonamer, which is followed by aggregation and growth in the *b* direction. Four nonamers stacked along *b* give rise finally to one nanoslab with dimensions of $1.3 \times 4 \times 4$ nm in the *a*, *b* and *c* crystallographic directions, respectively.

In the last paper of this series, Jacobs and coworkers[66] have studied the transformation of the nanoslabs into colloidal silicalite-1 crystals at 100 °C with *in-situ* low angle and wide angle X-ray scattering. The XRS patterns evidence the presence of three particle populations during the zeolite crystallization: nanoslabs (<3.7 nm), intermediates (5.7–13 nm) and large particles (>14.5 nm). The sizes determined for both intermediates and large particles are consistent with the presence of slabs which are multiples of the nanoslabs. Moreover, during the first hours of crystallization the initial amount of nanoslabs (around 70% of the overall silica) decreases exponentially in favour of the intermediates. At longer synthesis times, the intermediate concentration passes through a maximum, whereas the amount of large particles starts increasing. As soon as these large particles are detected, Bragg scattering is observed, which indicates that they are crystalline units. The above facts point towards an aggregation mechanism to explain the growth of the silicalite-1 crystals from the nanoslabs. According to the model depicted in Fig. 21, the aggregation of four nanoslabs leads to a tablet. Stacking of these tablets along the *a* direction gives rise to column-like intermediates. Finally, the zeolite crystals are proposed to be formed by aggregation and packing of the intermediates.

This mechanism has been also proposed to explain the crystallization of silicalite-2 (MEL topology) from clear solutions with TBA^+ cations as structure-directing agent.[65] The formation of a trimer leading to the MEL structure seems to follow the same path as for the MFI topology, although the authors conclude that in this case the subsequent trimer aggregation to form nanoslabs is more hindered. The existence of unfavourable TBA–TBA interactions suppresses the growth

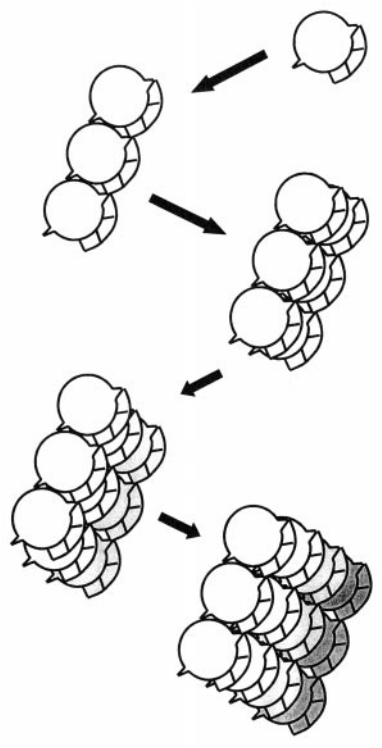

Fig. 20 Proposed mechanism of nanoslab formation by aggregation in the crystallization of silicalite-1 from clear solutions. Reprinted with permission from reference 65.

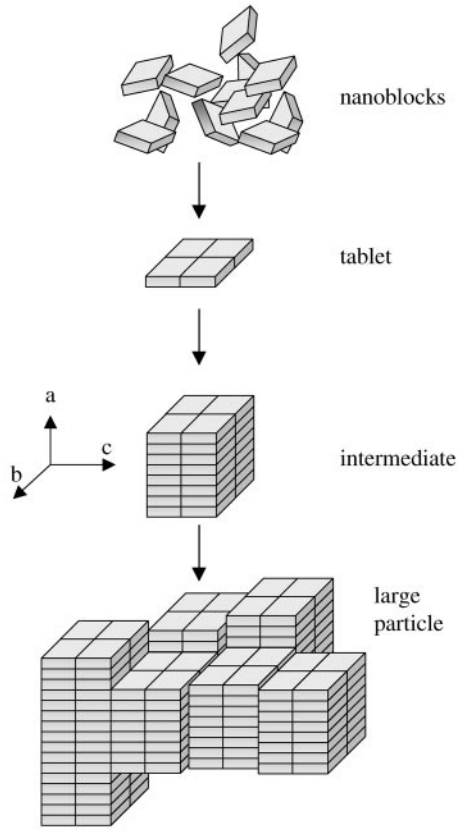

Fig. 21 Proposed mechanism for the formation of silicalite-1 crystals by aggregation of nanoslabs. Redrawn with permission from reference 66.

by aggregation along the *a* and *b* directions, whereas a double nanoslab is formed by connection along the *c* direction of the MEL structure.

Heterogeneous events have been also observed during the preparation of silicalite-1 films from clear solutions. Thus, Nakazawa *et al.*[67] have investigated the early stages of the crystallization of silicalite-1 films using field emission scanning electron microscopy (FE-SEM). The starting clear synthesis solution was prepared from TEOS, TPAOH, NaOH and water, being contacted at 175 °C with a quartz substrate located 2 cm below the gas/liquid interface. At short synthesis times (0.5 h), a gel layer is formed on both sides of the substrate. XPS measurements show the presence of N atoms in the gel layer, which is considered an indication of the presence of TPA^+ cations. After 1 h of heating, spherical particles with sizes around 10 nm are observed in the layer, that subsequently grow until reaching diameters in the range 10–20 nm. At long synthesis times, the formation of two populations of zeolite crystals on the quartz support takes place, which is explained by two different crystallization mechanisms that occur simultaneously. According to mechanism A, the nucleation step occurs directly within the nanoparticles of the amorphous gel phase, whereas the subsequent crystal growth takes place by incorporation of species from the solution, which leads to the formation of large and oriented silicalite-1 crystals (20 μm). By contrast, in mechanism B both nucleation and crystal growth steps are directly related to the nanoparticles. The FE-SEM images indicate that in this pathway the zeolite crystals are formed by aggregation and zeolitization of the nanoparticles, which results in the formation of small crystals (50–100 nm).

3.3. Crystallization of titanium-containing zeolites

This last section deals with several recent reports devoted to the investigation of the crystallization mechanism of zeolites having both Si and Ti atoms occupying framework positions. These reports have been focused on zeolites TS-1 and TS-2, which are the Ti-containing analogous of silicalite-1 and silicalite-2, respectively. As pointed out above for aluminosilicate zeolites, the presence of Ti in these materials as a T atom in addition to Si may be used as a probe for the crystallization mechanism. Characterization of Ti-containing zeolites by a number of techniques has led to the conclusion that the Ti atoms present a tetrahedral coordination in the zeolite lattice. By contrast, in amorphous SiO_2–TiO_2 solids, the Ti species may exhibit both tetrahedral and octahedral coordination. This fact provides an useful tool for discriminating between crystalline and amorphous titanosilicates.

The species and particles present in the raw clear solution for the synthesis of zeolite TS-1 have been isolated and characterized by Ravishankar *et al.*[68] This solution was obtained using TEOS and TBOT (tetrabutyl orthotitanate) as Si and Ti sources, whereas TPAOH was employed as structure-directing agent. The procedure for isolating the nanoparticles in the starting solution was similar to that described earlier for silicalite-1.[63] The solid obtained was formed by particles with sizes around 2–3 nm. The FTIR spectra showed a band in the region 550–590 cm^{-1}, typical of the MFI structure, which suggests the crystalline nature of the nanoparticles. TG analysis showed the presence of TPA cations in these particles. A variety of attempts to remove the template by calcination resulted in a partial collapse of the structure. The DR UV–Vis spectrum exhibits an absorption maximum below 250 nm, usually assigned to Ti atoms tetrahedrally coordinated to the silica framework. Nevertheless, some absorption is observed at higher wavelengths, indicating the presence also of Ti species with octahedral coordination, which is assigned by the authors to the insertion of water ligands in the Ti sites. A sample consisting of nanoparticles partially free of TPA molecules was obtained by calcination at low temperature and was used as a catalyst for phenol hydroxylation and hex-1-ene epoxidation with hydrogen peroxide. The conversions and selectivities obtained in both reactions were very similar to those for zeolite TS-1. From these results, the authors propose that the nanoparticles present in the raw clear solution are crystalline entities with the MFI zeolite structure, which is in agreement with the conclusions derived by this group for the crystallization of silicalite-1 and silicalite-2.

The synthesis of TS-1 from clear solutions has been also investigated by Uguina *et al.*[69,70] using both conventional and microwave heating. In the latter case, the use of microwave radiation allowed highly crystalline TS-1 samples to be synthesized in just 15 min. For both heating methods, the formation of an X-ray amorphous solid phase was detected in the earlier stages, this disappearing as the crystallization of zeolite TS-1 progressed. TEM images showed that the amorphous phase consists of particles with sizes in the range 8–15 nm, while XRF and TG analyses confirmed the presence of Ti species and TPA cations in these nanoparticles. The evolution of the TS-1 crystallinity with synthesis time was determined from both XRD and FTIR measurements, a similar trend being obtained in both cases. Since the IR band at 550 cm^{-1} is a measurement of the presence of the MFI structure, this result suggests that the nanoparticles in the precursor solid phase are mainly amorphous and that their lack of X-ray diffraction properties is not simply due to their small size. Likewise, the DR UV–Vis spectra of partially crystalline samples exhibited a strong absorption in the region 250–300 nm, indicating the presence of octahedral Ti species, probably located in the amorphous particles. TEM and SEM images taken on samples with different crystallinity showed that the TS-1 crystals are formed by a series of aggregation–zeolitization steps starting from the nanoparticles and leading to secondary particles with sizes increasing from 60 up to 120 nm. Fig. 22 illustrates a TEM micrograph of a partially crystalline sample that clearly evidences a mechanism of TS-1 crystal growth by aggregation of nanoparticles in this system. Nevertheless, in the last stages of the crystallization, the participation of soluble titanosilicate species is also suggested to yield the final TS-1 crystals.

A similar picture has been proposed for the crystallization of zeolite TS-2 from clear solutions under both conventional and microwave heating.[71] The formation of an X-ray amorphous phase consisting of titanosilicate species is observed in a first step previous to the detection of any crystalline material. The building blocks of this amorphous phase are again nanoparticles with sizes around 10–15 nm. TG analyses indicate the

Fig. 22 TEM image of a partially crystalline sample obtained in the crystallization of zeolite TS-1 from clear solutions.

presence of TBA^+ cations occluded within the amorphous phase, whereas N_2 and Ar adsorption measurements carried out on the calcined samples show that a large amount of micropores exist in the nanoparticles. The Ti atoms are located with both tetrahedral and octahedral coordination in the amorphous solid phase, as concluded from the DR UV–Vis spectra. However, some differences are observed in regards to the TS-1 crystallization when the samples were investigated by SEM and TEM. Thus, the nanoparticles are not completely independent but, even at short synthesis times, they are packed into larger particles of micrometer size. Moreover, some structural changes occur for the amorphous phase prior to the formation of zeolite crystals. The nanounits undergo an aggregation process to yield secondary particles with sizes around 200–300 nm, which are clearly seen to emerge from the surface of the macroparticles. In a further step, TS-2 polycrystals are formed directly from the secondary particles. These transformations take place initially without significant changes in the yield or in the Si/Ti ratio of the solid phase, hence the participation of soluble species is discarded, at least until reaching crystallinities around 50%. Beyond this value, both the solid yield and the Ti content increase, which is related to the incorporation of soluble species. Therefore, in this case the mechanism proposed for the crystallization of TS-2 from clear solutions involves both heterogeneous and homogeneous transformations.

4. Conclusions

Zeolite crystallization is a complex process that may take place through different pathways depending on the structure being synthesized, the gel composition and the synthesis conditions. While for many years, it has been assumed that the crystallization of zeolites is mainly a solution-mediated phenomenon, recent works point towards the existence of heterogeneous transformations, involving solid phases, in both nucleation and crystal growth steps.

In those syntheses starting from a solid-containing gel, the participation of the raw amorphous solid phase in the crystallization has been clearly established. Nucleation has been proposed to occur on the surface or even within the solid gel particles (autocatalytic mechanism). Moreover, in some cases the formation of the zeolite crystals has been observed to take place by reorganization of the amorphous phase (hydrogel) through solid–solid transformations, with little participation of soluble species. Aggregation and zeolitization of the amorphous particles, consisting of nanometer size units, have been proposed to explain the formation and growth of the zeolite crystals. In other cases, the amorphous hydrogel seems to be formed by non-isolated entities, with sizes also in the nanometer scale, which through a densification process lead to the zeolite crystals.

In zeolite syntheses starting from clear solutions, light scattering techniques have been recently applied as *in situ* measurements of the crystallization. In these systems, the absence of macroscopic solid phases led initially to the assumption that the crystallization occurs through a purely homogeneous mechanism. However, in many cases the formation of an X-ray amorphous gelatinous phase is observed prior to the detection of the first zeolite crystals. This solid phase is formed by particles with sizes below 10 nm (subcolloidal particles, nanoparticles, nanoslabs, *etc*). These particles are also present in the raw synthesis solution, which indicates that they are formed at room temperature prior to the hydrothermal crystallization. The existence of micropores in the nanoparticles, as well as the presence of organic molecules that act as structure-directing agents suggest that they are directly involved in the crystallization mechanism. The formation of nanoparticles and, subsequently, of aggregates seems to be a general pathway, as has been observed in the crystallization of different zeolite structures, for a variety of chemical compositions and in the presence of different structure-directing agents.

However, the exact nature of the nanoparticles remains still unclear. According to some authors these nanounits are amorphous since they do not exhibit any X-ray diffraction properties. However, other groups propose that the nanoparticles present an almost perfect crystalline structure, the absence of Bragg diffraction being attributed to their small size. A third alternative that should be also taken into account is the possibility that these nanoparticles have features intermediate between those of amorphous materials and perfectly crystalline entities. In this manner, it has been suggested that the nanoparticles are formed by a crystalline core surrounded by a partially amorphous shell. The presence of a high proportion of defects and water in the shells is assumed to promote their further fusion and growth.

Another common feature of many recent reports is the fact that the zeolite crystallization proceeds in many cases through aggregation steps involving primary or even secondary particles. In some cases, the whole crystallization process seems to be governed by the aggregation of particles with sizes mainly in the range 1–50 nm. However, in other cases aggregation is considered to be the main pathway during the formation of the zeolite nuclei, whereas the crystal growth is assumed to take place by incorporation of isolated nanoparticles to the growing crystals.

The crystallization of zeolites through heterogeneous *versus* homogeneous pathways may be also determined by the composition of the synthesis mixture. Thus, in those systems with a high concentration of solid phases, the occurrence of heterogeneous transformations seems to be favoured. This is so for syntheses carried out from wetness impregnated amorphous xerogels, crystallizations according to the dry gel method, and preparation of zeolitic membranes by vapour phase transport of both water and template molecules. The basicity of the reaction mixture is also a parameter that may strongly affect the crystallization mechanism as it determines the solubility of the silicate and aluminosilicate species. Under strongly basic conditions, the high solubility of silica promotes the participation of soluble species leading to a homogeneous crystallization. By contrast, heterogeneous mechanisms may occur in the crystallization of zeolites through the fluoride route due to the low solubility of silica at the neutral pH of the synthesis mixture. Likewise, in some cases the zeolite crystallization does not take place by a pure homogenous or heterogeneous pathway, but rather both contributions may occur simultaneously. Thus, different zeolite syntheses have been found to proceed mainly by the reorganization of solid phases during the earlier stages of the crystallizations, whereas the incorporation of soluble species becomes significant at the end of the crystal growth.

In spite of the progress achieved in recent years on the understanding of zeolite crystallization, a number of matters must still be investigated and clarified. The exact nature of the nanounits, that appear as precursors in most zeolite syntheses, need to be determined. Likewise, the extension of aggregation phenomena during both nucleation and crystal growth should be established. While most of the works published in recent years have been focused on the crystallization of pure silica zeolites, further studies are necessary to find out whether the observed heterogeneous transformations are modified when other species, such as Al, Ti, Ga, B, *etc.* are involved in the synthesis.

Finally, regarding the experimental methods used for the study of the crystallization mechanism, it has been suggested that the most valuable tools are *in situ* techniques as they do not modify the species and particles present in the synthesis medium. However, the information that can be derived from these direct methods is limited, hence probably the

combination of both *in situ* and *ex situ* measurements is necessary to achieve a complete understanding of the whole process of zeolite crystallization.

Acknowledgements

The authors gratefully acknowledge Comunidad de Madrid for financial support through the project ''Grupos Estratégicos de Investigación''.

References

1 A. Cronstedt, *Akad. Handl. Stockholm*, 1756, **18**, 120.
2 J. M. Garcés, *Proceedings of the 12th International Zeolite Conference*, ed. M. M. J. Treacy, B. K. Marcus, M. E. Bisher and J. B. Higgins, Materials Research Society, Warrendale, 1999, p. 551.
3 C. T. Kresge, M. E. Leonowicz, W. J. Roth, J. C. Vartuli and J. S. Beck, *Nature*, 1992, **359**, 710.
4 R. Szostak, *Molecular Sieves. Principles of Synthesis and Identification*, Van Nostrand Reinhold, New York, 1989, p. 190.
5 R. W. Thompson, in *Molecular Sieves. Science and Technology, vol. 1 Synthesis*, ed. H. G. Karge and J. Weitkamp, Springer-Verlag, Berlin, 1998, p. 1.
6 P. A. Jacobs, E. G. Derouane and J. Weitkamp, *J. Chem. Soc., Chem. Commun.*, 1981, 591.
7 E. G. Derouane, S. Detremmerie, Z. Gabelica and N. Blom, *Appl. Catal.*, 1981, **1**, 101.
8 Z. Gabelica, E. G. Derouane and N. Blom, in *Catalytic Materials: Relationship between Structure and Reactivity*, ed. T. E. Whyte, Jr., R. A. Dalla Betta, E. G. Derouane and R. T. K. Baker, ACS Symp. Ser. No. 248, American Chemical Society, Washington DC, 1984, p. 219.
9 P. Bodart, J. B. Nagy, Z. Gabelica and E. G. Derouane, *J. Chim. Phys. Biol.*, 1986, **83**, 777.
10 I. I. Ivanova, R. Aiello, J. B. Nagy, F. Crea, E. G. Derouane, N. Dumont, A. Nastro, B. Subotic and F. Testa, *Microporous Mater.*, 1994, **3**, 245.
11 B. Subotic, A. M. Tonejc, D. Bagovic, A. Cizmek and T. Antonic, *Stud. Surf. Sci. Catal.*, 1994, **84**, 259.
12 J. B. Nagy, I. Ivanova, R. Aiello, F. Crea, A. Nastro and F. Nesta, *Zeolites*, 1995, **15**, 421.
13 D. M. Ginter, A. T. Bell and C. J. Radke, *Zeolites*, 1992, **12**, 742.
14 B. Subotic and A. Graovac, *Stud. Surf. Sci. Catal.*, 1985, **24**, 199.
15 G. Golemne, A. Nastro, J. B. Nagy, B. Subotic, F. Crea and R. Aiello, *Zeolites*, 1991, **11**, 776.
16 S. P. Zhdanov, *Adv. Chem. Ser.*, 1971, **101**, 20.
17 J. Bronic and B. Subotic, *Microporous Mater.*, 1995, **4**, 239.
18 R. W. Thompson, *Zeolites*, 1992, **12**, 837.
19 S. Gonthier, L. Gore, I. Güray and R. W. Thompson, *Zeolites*, 1993, **13**, 414.
20 X. Wenyang, L. Jianquan, Li Wenyuan, Z. Huiming and L. Bingchang, *Zeolites*, 1989, **9**, 468.
21 W. Fan, R. Li, B. Fan, J. Ma and J. Cao, *Appl. Catal.*, 1996, **143**, 299.
22 W. Xu, J. Dong, J. Li, J. Li and F. Wu, *J. Chem. Soc., Chem. Commun.*, 1990, 755.
23 M. H. Kim, H. X. Li and M. E. Davis, *Microporous Mater.*, 1993, **1**, 191.
24 M. Matsukata, N. Nishiyama and K. Ueyama, *Microporous Mater.*, 1993, **1**, 219.
25 P. R. Hari Prasad Rao, K. Ueyama and M. Matsukata, *Appl. Catal. A*, 1998, **166**, 97.
26 J. Dong, T. Dou, X. Zhao and L. Gao, *J. Chem. Soc., Chem. Commun.*, 1992, 1056.
27 M. Matsukata, N. Nishiyama and K. Ueyama, *Microporous Mater.*, 1996, **7**, 109.
28 W.-Y. Dong, Y.-J. Sun, H.-Y. He and Y.-C. Long, *Microporous Mesoporous Mater.*, 1999, **32**, 93.
29 S. Yamazaki and K. Tsutsumi, *Microporous Mesoporous Mater.*, 2000, **37**, 67.
30 S. L. Burkett and M. E. Davis, *J. Phys. Chem.*, 1994, **98**, 4647.
31 L. W. Beck and M. E. Davis, *Microporous Mesoporous Mater.*, 1998, **22**, 107.
32 J. Warzywoda, R. D. Edelman and R. W. Thompson, *Zeolites*, 1991, **11**, 318.
33 M. A. Camblor, A. Corma and S. Valencia, *Chem. Commun.*, 1996, 2365.
34 D. P. Serrano, R. van Grieken, P. Sánchez, R. Sanz and L. Rodríguez, *Microporous Mesoporous Mater.*, 2001, **46**, 35.
35 M. A. Uguina, G. Ovejero, R. van Grieken, D. P. Serrano and M. Camacho, *J. Chem. Soc., Chem. Commun.*, 1994, 27.
36 D. P. Serrano, M. A. Uguina, G. Ovejero, R. van Grieken and M. Camacho, *Microporous Mater.*, 1995, **4**, 273.
37 D. P. Serrano, M. A. Uguina, G. Ovejero, R. van Grieken and M. Camacho, *Microporous Mater.*, 1996, **7**, 309.
38 D. P. Serrano, M. A. Uguina, G. Ovejero, R. van Grieken and M. Camacho, *Chem. Commun.*, 1996, 1097.
39 M. A. Uguina, D. P. Serrano, G. Ovejero, R. van Grieken and M. Camacho, *Zeolites*, 1997, **18**, 368.
40 M. Shibata, J. Gérard and Z. Gabelica, *Microporous Mater.*, 1997, **12**, 141.
41 J. A. Melero, R. van Grieken, D. P. Serrano and J. J. Espada, *J. Mater. Chem.,*, 2001, **11**, 1519.
42 D. P. Serrano, M. A. Uguina, G. Ovejero, R. van Grieken, M. Camacho and J. Melero, *J. Mater. Chem.*, 1999, **9**, 2899.
43 L. Gora and R. W. Thompson, *Zeolites*, 1995, **15**, 526.
44 M. Tsapatsis, M. Lovallo and M. E. Davis, *Microporous Mater.*, 1996, **5**, 381.
45 O. Regev, Y. Cohen, E. Kehat and Y. Talmon, *Zeolites*, 1994, **14**, 314.
46 R. van Grieken, J. L. Sotelo, J. M. Menéndez and J. A. Melero, *Microporous Mesoporous Mater.*, 2000, **39**, 135.
47 T. A. M. Twomey, M. Mackay, H. P. C. E. Kuipers and R. W. Thompson, *Zeolites*, 1994, **14**, 162.
48 A. E. Persson, B. J. Schoeman, J. Sterte and J.-E. Otterstedt, *Zeolites*, 1994, **14**, 557.
49 B. J. Schoeman, J. Sterte and J.-E. Otterstedt, *Zeolites*, 1994, **14**, 568.
50 B. J. Schoeman, *Zeolites*, 1997, **18**, 97.
51 B. J. Schoeman and O. Regev, *Zeolites*, 1996, **17**, 447.
52 B. J. Schoeman, *Microporous Mater.*, 1997, **9**, 267.
53 B. J. Schoeman, *Stud. Surf. Sci. Catal.*, 1997, **105**, 647.
54 B. J. Schoeman, *Microporous Mesoporous Mater.*, 1998, **22**, 9.
55 W. H. Dokter, H. F. van Garderen, T. P. M. Beelen, R. A. van Santen and W. Brass, *Angew. Chem., Int. Ed. Engl.*, 1995, **34**, 73.
56 P.-P. E. A. de Moor, T. P. M. Beelen and R. A. van Santen, *Microporous Mater.*, 1997, **9**, 117.
57 P.-P. E. A. de Moor, T. P. M. Beelen, B. U. Komanschek, O. Diat and R. A. van Santen, *J. Phys. Chem. B*, 1997, **101**, 11077.
58 P.-P. E. A. de Moor, T. P. M. Beelen and R. A. van Santen, *J. Phys. Chem. B*, 1999, **103**, 1639.
59 P.-P. E. A. de Moor, T. P. M. Beelen, R. A. van Santen, L. W. Beck and M. E. Davis, *J. Phys. Chem. B*, 2000, **104**, 7600.
60 P.-P. E. A. de Moor, T. P. M. Beelen, R. A. van Santen, K. Tsuji and M. E. Davis, *Chem. Mater.*, 1999, **11**, 36.
61 J. N. Watson, L. E. Iton and J. W. White, *Chem. Commun.*, 1996, 2767.
62 J. N. Watson, L. E. Iton, R. I. Keir, J. C. Thomas, T. L. Dowling and J. W. White, *J. Phys. Chem. B*, 1997, **101**, 10094.
63 R. Ravishankar, C. E. A. Kirschhock, P.-P. Knops-Gerrits, E. J. P. Feijen, P. J. Grobet, P. Vanoppen, F. C. De Schryver, G. Miehe, H. Fuess, B. J. Schoeman, P. A. Jacobs and J. A. Martens, *J. Phys. Chem. B*, 1999, **103**, 4960.
64 C. E. A. Kirschhock, R. Ravishankar, F. Verspeurt, P. J. Grobet, P. A. Jacobs and J. A. Martens, *J. Phys. Chem. B*, 1999, **103**, 4965.
65 C. E. A. Kirschhock, R. Ravishankar, L. Van Looveren, P. A. Jacobs and J. A. Martens, *J. Phys. Chem. B*, 1999, **103**, 4972.
66 C. E. A. Kirschhock, R. Ravishankar, P. A. Jacobs and J. A. Martens, *J. Phys. Chem. B*, 1999, **103**, 11021.
67 T. Nakazawa, M. Sadakata and T. Okubo, *Microporous Mesoporous Mater.*, 1998, **21**, 325.
68 R. Ravishankar, C. Kirschhock, B. J. Schoeman, D. De Vos, P. J. Grobet, P. A. Jacobs and J. A. Martens, *Proceedings of the 12th International Zeolite Conference*, ed. M. M. J. Treacy, B. K. Marcus, M. E. Bisher and J. B. Higgins, Materials Research Society, Warrendale, 1999, p. 1825.
69 M. A. Uguina, D. P. Serrano, R. Sanz and E. Castillo, *Proceedings of the 12th International Zeolite Conference*, ed. M. M. J. Treacy, B. K. Marcus, M. E. Bisher and J. B. Higgins, Materials Research Society, Warrendale, 1999, p. 1917.
70 M. A. Uguina, D. P. Serrano, R. Sanz, A. Rodríguez and E. Castillo, in preparation.
71 D. P. Serrano, M. A. Uguina, R. Sanz, P. Sánchez and E. Castillo, in preparation.